European School of Molecular Medicine

Sede di Napoli

BIOTECNOLOGIE AVANZATE
"LISTENING TO BIOMOLECULES TO SILENCE DISEASE"

EUROPEAN SCHOOL OF MOLECULAR MEDICINE

SEMM SITE: NAPLES

UNIVERSITA' DEGLI STUDI DI NAPOLI "FEDERICO II"

Ph.D. in Molecular Medicine – Ciclo XXI
Human Genetics

"PHENYLKETONURIA: FROM THE CHARACTERIZATION OF NEW MUTATIONS TO THE CORRECTION OF THE PATHOLOGIC PHENOTYPE BY A HELPER-DEPENDENT ADENOVIRAL VECTOR EXPRESSING PAH "

Tutor:
Prof. Francesco Salvatore

Internal Supervisor:
Prof. Lucio Pastore

External Supervisor:
Prof. Brendan Lee

Coordinator:
Prof. Francesco Salvatore

Ph.D. student:
Dr Monica Cerreto

Accademic Year: 2008-2009

CHAPTER 1 – INTRODUCTION

CHAPTER 2 – MATERIALS AND METHODS

CHAPTER 1

INTRODUCTION

1. INTRODUCTION

1.1 Phenylketonuria: the PAH gene and enzyme and the disease-causing mutations

Phenylketonuria (PKU) is one of the most common inherited metabolic diseases (IEM). The incidence is approximately 1:10,000 Caucasian live births (OMIM 261600) and is caused by a deficient activity of phenylalanine hydroxylase (PAH; EC 1.14.16.1), a non-heme iron-dependent enzyme that catalyzes the hydroxylation of L-phenylalanine (L-Phe) to L- tyrosine (L-Tyr) in the presence of (6*R*)-L-erythro-5,6,7,8-tetrahydrobiopterin (BH4) and molecular dioxygen as cosubstrates (1) **(Figure 1)**.

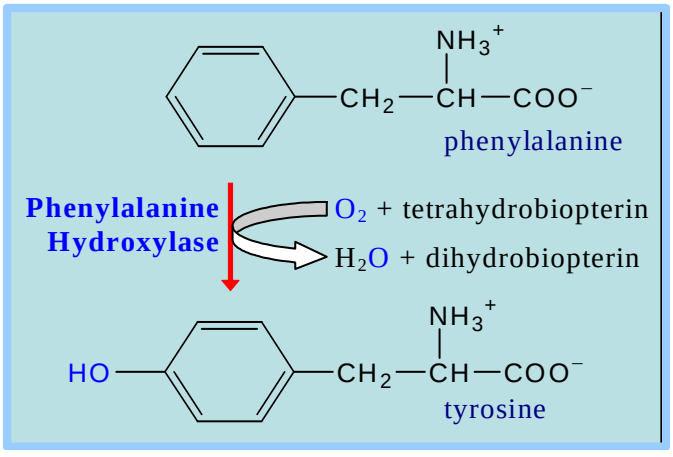

Figure 1: Reaction catalyzed by the PAH. The enzyme PAH converts Phe to Tyr using BH4 and oxygen. BH4 is recycled via a two-step pathway which utilizes NADH.
The PAH gene contains 13 exons and maps on chromosome 12q22-q24.1.

The enzyme assembles into homotetramers, with each subunit consisting of three domains: an N-terminal regulatory domain (residues 1–142), a large catalytic domain (residues 143–410) and a C-terminal domain (residues 411–452) that is responsible for tetramerization and includes a dimerization motif (411–426) (1) **(Figure 2)**.

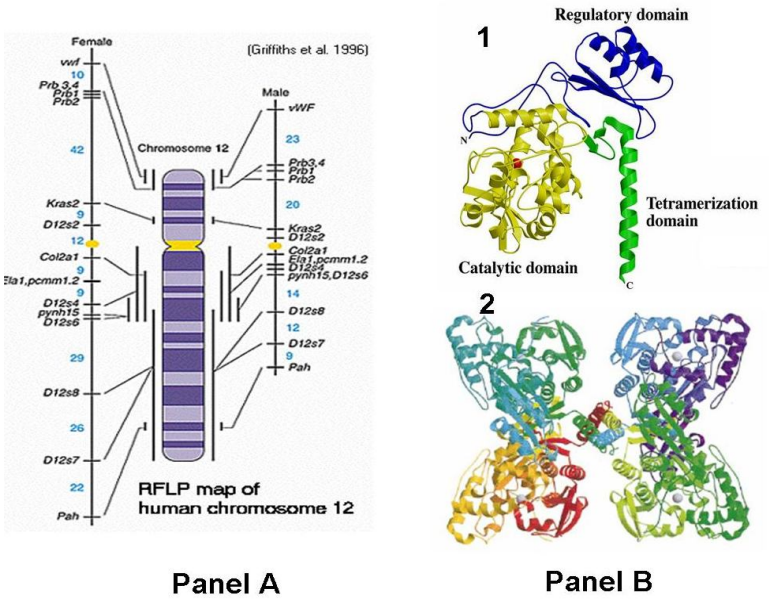

Figure 2: PAH gene and enzyme. The PAH gene maps onto chromosome 12q22-q24.1 (Panel A). Each PAH monomer consists of an N-terminal regulatory domain (blue), a large catalytic domain (yellow) and a C-terminal domain (green) (Panel B,1). The active enzyme derives from the association of 4 monomers (Panel B,2).

In humans, liver PAH activity provides L-Tyr for protein and neurotransmitter biosynthesis, it is involved in energy metabolism, and most importantly, it prevents plasma L-Phe accumulation, which is toxic to the brain (2,3).

As a consequence, a defective activity of PAH leads to hyperphenylalaninemia (HPA), that, according to the magnitude of the increase in blood Phe, can be classified as: mild HPA (MHP), mild or variant PKU and classical PKU (1).

The defective activity of PAH depends on mutations of the PAH gene.

To date, more than 500 disease-causing mutations have been discovered and are listed in PAHdb at http://www.pahdb.mcgill.ca/. The majority of these are scattered over the entire gene length but with a different frequency in distinct populations and geographic areas (4-9) and a number of them have been analyzed and characterized (10-12). Thanks to these studies, it is now known that most of PAH missense mutations result in a misfolding of the protein which increases its turnover both *in vitro* and probably *in vivo*, pointing to a decreased conformational stability as the major molecular mechanism for the loss of PAH function in PKU (13).

Recently, it has been discovered that some PAH mutations are responsive to BH4 treatment. These mutations show a residual enzymatic activity that is associated with BH4 responsiveness (14-15). Patients with these mutations show an improvement in their clinical conditions after oral administration of BH4 because their mutant enzymes suppress the low binding affinity for BH4, enabling the L-

Phe hydroxylation reaction. Most of these BH4-responsive PAH mutations map to the catalytic domain of PAH, in cofactor-binding regions or in regions that interact with the secondary structural elements involved in cofactor binding.

In a small cohort of HPA patients, no PAH mutations have been found and the disease has been related to a lack of the BH4, due to defective cofactor biosynthesis and regeneration. This group, however, represents only 1% of all HPA cases (16).

1.2 PKU brain pathology

In most industrialized countries, HPA is diagnosed during newborn screening programs (17), with a remarkable success in preventing the major manifestations of the disease that, as stated above, are due to brain injuries.

In fact, L-Phe accumulation is associated with a phenotype presenting with growth failure, microcephaly, seizures, and mental retardation (2,3).

To date, despite the large number of studies, the pathogenesis of brain dysfunction in PKU is still unclear. However, it is known that L-Phe interferes with various cerebral enzyme systems, such as tyrosine hydroxylase and tryptophan hydroxylase, influencing neurotransmitter synthesis (18) and causing a decrease of brain amine contents (19), as well as HMG-CoA reductase, thus resulting in impaired cholesterol synthesis (20). High concentrations of L-Phe have also been

related to a reduction of glutamatergic and glutaminergic synaptic transmissions (21,22), synaptogenesis and activity of the pyruvate kinase enzyme(23).

Other studies have shown that glucose metabolism is low in the brain of phenylketonuric patients, so altering the normal energy metabolism (24,25,26).

Moreover, increased levels of L-Phe seems also to cause a reduction of the other large neutral aminoacids (LNAA), probably because of a competition for the same transporter through the blood brain barrier (27-31).

To complete this overview on PKU brain pathology, recent *in vitro* and *in vivo* studies have highlighted a role of oxidative damage elicited by L-Phe and its derivates in rat brain (32).

1.3 PKU maternal syndrome

Another problem associated with PKU is the so called maternal syndrome. This syndrome is caused by high L-Phe levels during pregnancy and presents an incidence of 1/30000-40000 gestations. Increasing levels of L-Phe in pregnant PKU women cause severe teratogenic effects in the fetuses that can develop microcephaly, mental retardation (75-90%) and congenital heart disease (15%) (33) **(Figure 3)**.

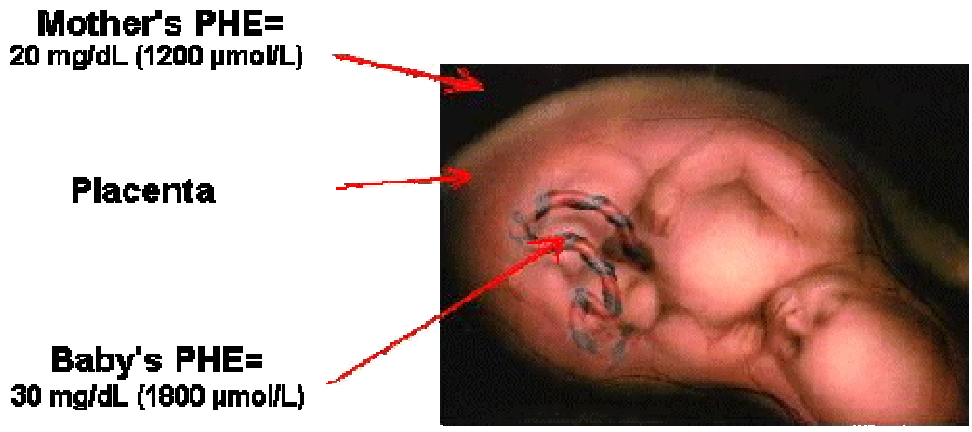

Figure 3: Maternal PKU syndrome. The maternal syndrome derives from the exposition of the fetus to the maternal elevated Phe levels that cross the placental barrier causing birth defects.

Many hypothesis regarding the pathogenesis of PKU maternal syndrome have been proposed: some authors believe that the damage is due to the transport of aminoacids across the placental barrier (34), whereas others focus on the direct damage of alternative products of L-Phe metabolism on fetal organs (35).

According to the first hypothesis, fetuses may lack sufficient aminoacids to perform an optimal protein synthesis because excessive amounts of L-Phe inhibit the transport of aminoacids such as tyrosine, isoleucine, valine and methionin.

The second hypothesis instead is based on the damage deriving from the exposition of fetuses to alternative L-Phe metabolites such as phenylacetic acid, phenylethilamine or a combination of both. This second hypothesis reduces the role of L-Phe in the development of fetus abnormalities. By the way, some evidences seem to support the first hypothesis, consisting in the direct role of L-

Phe; in fact, analysing fetal tissues, it is possibile to observe that while L-Phe is present in great amounts, L-Phe metabolites are present only in minimal amounts. A major support to the first hypothesis is also given by the observation that women with defects in the accumulation of L-Phe metabolites have normal chidren. This demonstrates that L-Phe is the real teratogenic agent and that it causes fetal abnormalities alone or in association with its alternative metabolites.

As mentioned before, HPA is diagnosed in newborn screening programs (17) that avoiding the development of neuronal damage in babies born with PKU and allowing an increasing number of people with the disease to reach adulthood, to work and to form relationships. However, it is also evident that, thanks to this newborn screening, a greater number of healthy PKU women of child−bearing age exist. These women are at high risk of having babies with mental and physical impairments if they do not control their L-Phe levels. For this reason, PKU women must plan eventual gestations and, if they should decide to have children, they must consult specialized centres at least six months before gestation to discuss the treatment with experts. In fact, if the gestation has not been planned and L-Phe levels remain high in the first eight weeks, PKU women are at risk of having babies with severe defects which cannot be avoided even if L-Phe is strictly monitored (36).

1.4 PKU actual treatment: the low Phe diet

As stated in **1.2** and **1.3** sections, PKU related symptoms are severe, therefore it is necessary to treat this disease since birth.

At present, PKU is treated with a lifelong dietary protein restriction (37), in which many common foods, such as milk and dairy products, meat, eggs, wheat, beans, corn, peanuts, lentils, and other grains, are prohibited to the patients.

The diet consists of drinkable formulas, synthethically made as nutritional substitutes for all the eliminated foods, containing no Phe but all the necessary vitamins, minerals, aminoacids. Moreover, it allows low protein special foods and measured amounts of fruits, vegetables and grain products **(Figure 4).**

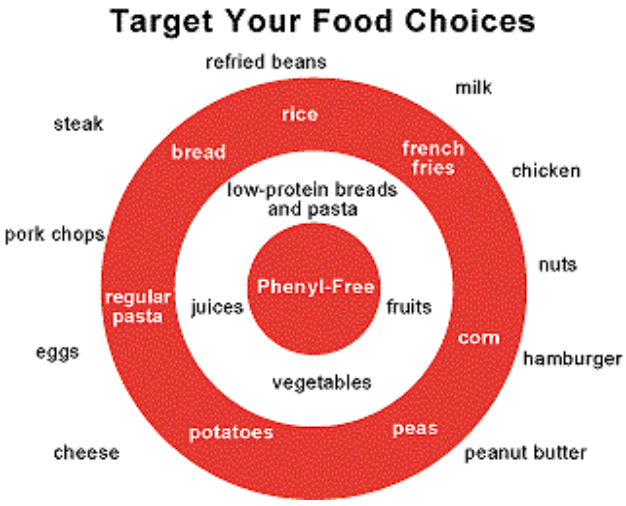

Figure 4: Low Phe diet. Foods that are allowed are in the inner part of the diagram (white circle).

CHAPTER 1- INTRODUCTION

In the past, it was common for children to be taken off the diet between 6 and 10 years of age, when brain development was considered to be completed, however, discontinuation of the diet resulted in many serious problems such as:

1. deterioration of intellectual quotient,
2. learning disabilities,
3. behavioural problems (hyperactivity, irritability, self abusing behaviours),
4. neurological impairments (severe tremors, epilepsy resistant to anticonvulsivant therapy, spastic paraparesis and quadriparesis with the risk of becoming wheel chair bound),
5. eczema,
6. personality disorders (schizophrenia, panic attacks).

It is now a common knowledge that dietary therapy must be followed for life but it has been shown that Phe levels within the recommended range are achieved by 70% of the children younger than 10 years but only by 20% of those 15 years and older.

Therefore, despite being a huge advance and generally effective, a low Phe diet cannot be considered the dream management for PKU patients, and a number of different approaches have been developed in the last few years towards an alternative treatment for PKU. Thanks to the availability of a good animal model for this pathology, it has been possible to experimentally explore new treatments

for PKU that, in some cases, seem to be really promising for the treatment of the disease.

1.5 PKU animal models

The first animal model that was proposed for PKU was represented by rats to which phenylalanine analogues had been administered as PAH inhibitors to suppress the enzyme activity**.** However, the results were complicated by side effects of these inhibitors (38). More successful was the chemical mutagenesis of a BTBR-mouse strain using the alkylating agent N-ethyl- N-nitrososurea (ENU) that resulted in the isolation of a hyperphenylalaninemic mouse with a mutation called Pahenu2 (39) **(Figure 5).**

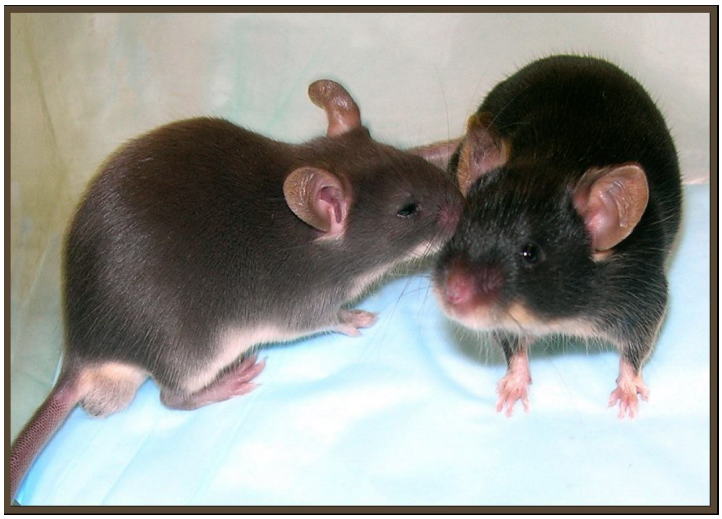

Figure 5: Murine model of PKU. Phenylketonuric mice are simply recognized for their characteristic greyish coat color (left side of the picture). Normal mice present a black coat (right side of the picture).

The Pahenu2 allele was genetically mapped to the Pah locus and sequence analysis revealed a missense mutation at exon 7, in the region encoding the active site of the enzyme, which is by far the most frequent mutation site for PKU in humans.

Besides hyperphenylalaninemia, this mouse presented many symptoms observed in PKU patients, namely: slow growth, small head, hypopigmentation, behavioural disturbances and maternal PKU syndrome (40,41). Genetics and biochemistry have demonstrated the reliability of this animal as model for human PKU .

Thus, most PKU-animal studies, if not all, in somatic gene therapy and enzyme replacement, have been carried out in this Pahenu2 mouse model and provided valuable information on the biology and pathology of PKU.

Besides these studies, focused on the discovery of new strategies to treat PKU, these mice have been also a model for investigating PKU brain pathology as they present a decrease of the amine contents from the thirth to the fifth week of life (42), impairments of the glutamatergic synaptic transmission (22), pathologic alterations in the hypothalamic and mesencephalic regions that begin at four weeks of age (43) and evidences of a reversible neurodegeneration in the nigro-striatal area at the same age (44).

Moreover, PKU mice also show a severe behavioural phenotype, with deficits involving both spatial and non-spatial recognition that are not related to motor impairments or to high emotional reactivity to novelty (45).

1.6 Alternatives approaches to PKU treatment

As mentioned in **1.4 section**, PKU related symptoms can be prevented by a strict dietary restriction from early infancy. Although it is recognized that dietary treatment initiated early in life is successful in avoiding the severe mental retardation of PKU, this treatment presents many limitations, since PKU patients must adhere to an unpalatable, expensive and lifelong diet (37) that is frequently stopped prematurely, leading to an unsatisfactory clinical outcome (33,46,47).

Therefore, alternatives to the diet such as protein substitutes with a more pleasant flavour (48), Phe-ammonia lyase administration (49), large neutral aminoacids supplementation (50) and gene therapy (51-55) have been proposed. In particular, gene therapy is a very promising approach for the treatment of PKU.

Several vectors have been used at this purpose including first generation adenoviral (FG−Ad) vectors, integrating vectors and adeno−associated vectors (AAV) (56).

FG−Ad vectors have been able to efficiently rescue the phenotype of PKU but for a very short period because of the strong immune response that followed their *in*

vivo administration (51,52). Fang et al. (51) used a recombinant adenoviral vector containing the human PAH-cDNA under control of the Rous sarcoma virus long-terminal repeat (RSV-LTR). The recombinant virus was injected into the liver through the portal vein of the PKU mouse. A complete normalization of the serum phenylalanine levels and a significant increase of PAH activity was obtained in these PKU mice within one week of treatment. Unfortunately, the therapeutic effect of the adenoviral vector delivery did not persist beyond a few weeks, and repeated administration did not reproduce the original results due to the neutralizing antibodies against the adenoviral vector. Furthermore, this study did not rescue other phenotypic changes such as for instance hypopigmentation. However, an important finding from this study was that 10–20% of normal PAH enzymatic activity was sufficient to restore normal serum phenylalanine levels.

In another study, a recombinant FG−Ad vector containing the strong CAG-hybrid promoter was constructed to drive expression of the human PAH gene in the PKU mouse to potentially enhance treatment efficacy (52). Also in this case, the therapeutic effect did not persist beyond few weeks but suppression of the host immune response by administration of the immunosuppressant FK506 allowed repeated gene delivery, resulting in moderately prolonged PAH gene expression and reversal of hypopigmentation.

Integrating vectors, on the other hand, have shown a prolonged duration of expression compared to FG−Ad vectors. An early approach that was done for

PKU treatment consisted of the transduction via recombinant retroviral vectors of the PAHcDNA into hepatocytes isolated from the PKU mouse (53,54). The PAH gene was efficiently transferred and expressed at high levels in these primary hepatocytes, however, the risk of mutagenesis for these vectors is unacceptable for a disease with an alternative diet therapy.

AAV vectors have, at the moment, provided the best results for gene therapy of PKU even if they present some limitations such as the small cargo capability, the need to find the right serotype to increase hepatocytes transduction and the different therapeutic response after the injection of the AAV vector between males and females. In fact, in initial trials (55), only male mice responded to the AAV mediated therapy by lowering phenylalanine to therapeutic levels, whereas females were unresponsive unless they were ovariectomized and treated with testosterone. This limitation was overcame with following studies (56), obtaining a normalization also in female mice, even though higher doses of the therapeutic vector were necessary to achieve a phenotypic correction.

1.7 The potential of adenoviral vectors as liver directed gene delivery systems

A crucial factor for the proposal of a gene therapy strategy to treat PKU is the choice of an appropriate vector. Each of the vectors currently used possesses a

unique set of characteristics that renders it most suited for specific applications in gene therapy.

In particular, among viral vectors, those deriving from adenoviruses seem to be really promising for the treatment of pathologies whose defect is in the liver. This particular feature derives from the natural tropism that adenoviruses show for hepatocytes after intravenous delivery (57). Numerous demonstrations of adenoviral vector-mediated delivery of a wide array of transgenes in several animal species and in humans have been reported and many examples of liver pathologies have been successfully treated by adenoviral vector-mediated gene therapy (58). In fact, many liver diseases lack satisfactory treatment and alternative therapeutic options are needed. A considerable number of preclinical studies indicate that a great variety of liver diseases, including inherited metabolic defects, chronic viral hepatitis, liver cirrhosis and primary and metastatic liver cancer, are amenable to gene therapy treatments with adenoviral vectors. Moreover, gene transfer to the liver can also be used to convert this organ into a factory of secreted proteins needed to treat conditions that do not affect the liver itself.

For all these reasons, the treatment of PKU with adenoviral vectors seems to be a very promising approach to cure this disease, especially because recent developments in these vectors have originated a very safe system (named helper

dependent adenoviral vectors) that is able to mediate high-efficiency transduction and to direct sustained high-levels of transgene expression with negligible chronic toxicity (59-60)

1.8 Adenoviruses

Adenoviral vectors derive from modifications of wild type adenoviruses. Adenoviruses were first discovered more then 50 years ago by Rowe and colleagues from human adenoid cells (61). They have a linear, double stranded DNA of about 36 kb surrounded by a protein structure with an icosahedral shape named capsid **(Figure 6)**.

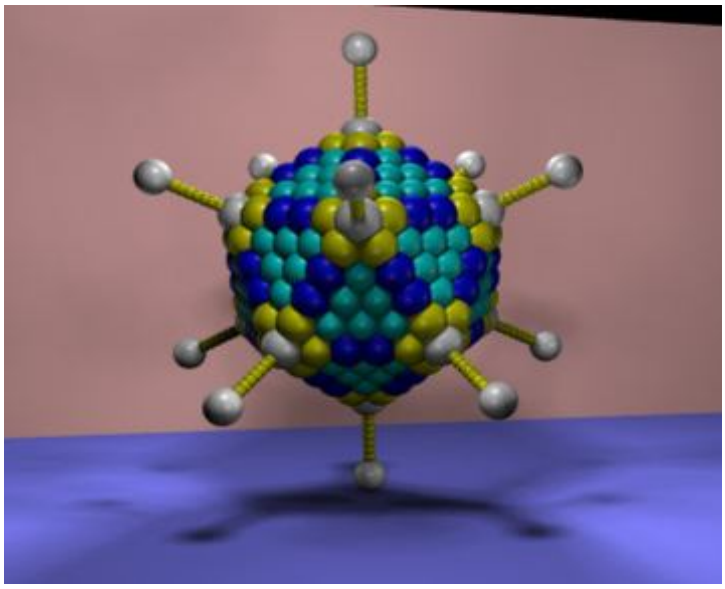

Figure 6: Adenovirus structure: a three-dimensional image reconstruction of Ad5.

CHAPTER 1- INTRODUCTION

The adenoviral virion is a non-enveloped particle about 70-90 nm in size with an outer protein shell (capsid) surrounding an inner nucleoprotein core. The icosahedral capsid consists of 252 capsomers divided in 240 hexons and 12 pentons. Each hexon is composed of three monomeric polypeptides (polypeptide II) forming the 20 triangular facets of the capsid; the penton, instead, shows a more complex structure, constituted by five monomeric polypeptides (polypeptide III), which act to anchor a trimeric protein, the fiber (polypeptide IV). The penton and the fiber form the penton complex that seals the capsid attach of the 12 virion vertices. These proteins are responsible for the attachment (fiber) and internalization (penton) of the virus into host cells.

The capsid is composed also of a number of other minor components including protein IIIa, pVI, pVIII and pIX. Adenovirus cores contain the viral genome, a linear, double strended DNA that is approximately 36 kb long. Each end of the genome has an inverted terminal repeat (ITR) of 100-140 bp with a terminal protein (TP) attached covalently (62). This protein protects the DNA from the endonucleases of the host cell. The genome is associated with other proteins like the basic protein VII and a small peptide termed *mu* (63), with the function to stabilize the DNA into the capsid. Another protein is packaged with the DNA, the protein V. This protein is attached to the genome on one side and on the other side to the capsid protein VI, so it links the viral DNA to the capsid (64). The virions contain also some copies of the adenovirus protease (Pr) that cleaves many of the

structural preproteins into their mature forms during the last stage of viral assembly.

Since their discovery, more then 100 different species of adenoviruses have been identified from various species. In particular, human adenoviruses are classified into 6 subgroups (A-F), which are further subdivided into 51 serotypes (65).

Among human adenoviruses, serotype 2 (Ad2) and serotype 5 (Ad5) of subgroup C are the most extensively studied.

Once in contact with the target cell the adenovirus infection proceeds through two phases **(Figure 7)**.

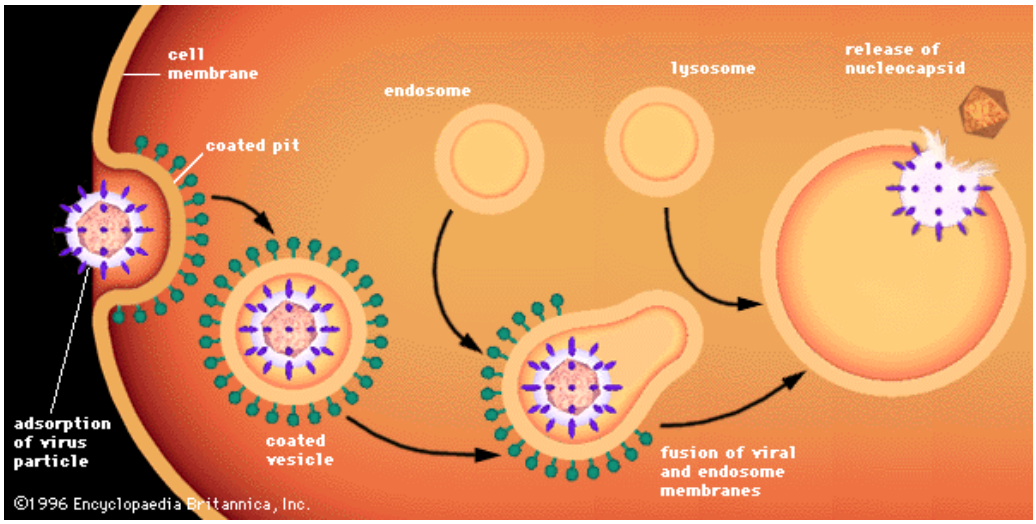

Figure 7: Adenovirus entry into the host. The adsorption of the virus to target cell receptors involves high-affinity binding via the knob portion of the fibre. The prime receptor for human Adenovirus serotype 5 is identical to that for coxsackie B virus and has been named the coxsackie/Adenovirus receptor (CAR). After the attachment step, interaction between the penton base and αv integrins on the cell surface leads to internalization of the virus through endocytosis.

The first is named “early” phase and occurs in 6-8 hours. This phase comprises the entry of the virus into the host cell, the passage of the viral genome into the cytoplasm to the nucleus, the internalization of the adenoviral DNA into the nucleus and the transcription and translation of some viral genes, named early genes. These events modulate the cell metabolism to facilitate the replication of the virus DNA. The second phase is the “late” phase which can take about 4-6 hours after the beginning of the transcription of the late genes. The initial attachment of the virion particles to the cell surface occurs through a high affinity binding between a portion of the fiber (*knob* domain) and a cell receptor. The first receptor identified was shown to be identical to that for Coxackie B virus and has therefore been termed Coxackie/adenovirus receptor (CAR) (66). CAR is a type I transmenbrane protein of 46 kDa belonging to the immunoglobulin superfamily which is present on the basolateral membrane of several epithelial cells in many tissues including heart, lung, liver and brain. All groups of adenoviruses use CAR for the adsorption of the virus to the target cell, except the adenoviruses of group B. These viruses bind another cellular receptor, the CD46, a complement regulatory protein. Therefore, the adenoviruses of group B are capable to infect some cells, like hematopoietic stem cells, dendritic cells and malignant tumor cells, which are resistant to the infection by the adenoviruses using CAR as the primary attachment receptor. All these data suggest that receptor recognition could be a key factor involved in cell tropism, to the point to to change it. The

adenovirus fiber can be modified by constructing chimeric viruses carrying fiber genes from different serotypes, or by binding the fiber with several antibodies (67 68). After the initial attachment of the fiber *knob* portion to the cell surface, an RGD motif, exposed on the penton base (69), interacts with cellular αv integrins (70), in presence of divalent cations. In particular, the heterodimeric integrins, αvβ3 and αvβ5, support the adenovirus internalization playing an important role in the determination of the tropism. The interaction between adenovirus and plasma membrane can induce the activation of several signaling pathways like that of phosphoinositide-3-OH kinase (PI-3K), which triggers the Rho family of GTPases with consequential polymerization of actin and cythoscletal reorganization (71). Another pathway, activated 20 minutes post infection, is the Raf/Mitogen-activated protein kinase (MAPK) pathway, which culminates in the production of interleuchin 8 (IL-8) (72). Together, these events induce the adenovirus internalization through a clathrin-mediated endocytosis. In the acidic environment of the endosome, the virus-encoded protease mediates the dismemberment of the viral capsid through the proteolysis of the protein VI, which induces, in turn, the escape of virions to the cytoplasm. The passage through the cytoplasm to the nucleus seems to be mediated by the cellular protein p32 (73), which binds the virus core (constituted by the DNA and its associated proteins TP, *mu*, proteins VII and V), and involves dynein and microtubules (74). One hour after the infection, it is possible to detect the virion on the nuclear

matrix, where TP forms a complex with the cellular CAD pyrimidine synthesis enzyme (75) and p32 binds the nuclear lamin B to permit the dissociation between the viral DNA and the linked proteins.

1.8.1 Early gene and DNA replication

The transcription of adenoviral genes can be divided in two phases, early and late, occurring before or after viral DNA replication. The first viral transcribed gene is E1, which encodes for two products: E1A and E1B, each of them producing multiple proteins by way of differential mRNA processing. Two E1A transcripts are produced during early infection, encoding the 289R protein and 243R protein. These proteins have the function to modulate the cellular metabolism to make the cell more susceptible to virus replication. In order to do this, they act as *trans*-activators on the other early adenovirus genes and induce the cells to enter in S phase (76). Indeed, both 289R and 243R protein are able to sequester Rb protein (Retinoblastoma protein), bounded to the transcriptional factor E2F, allowing the release of this factor and the activation of its target genes necessary for driving the cell into S phase (77). Moreover, E1A proteins can also bind proteins involved in the control of cell cycle, such as cyclin-dependent-kinase-inhibitor p21, or factors mediating chromatin structure like p400, pCAF and p300/CBP. The E1B gene product 55K (E1B-55K) acts blocking p53-dependent apoptosis by directly

binding p53, accumulated during cell cycle deregulation by E1A, and inhibiting its ability to induce expression of proapoptotic genes (78). Instead, the other product of E1B gene, E1B-19K, blocks the pathway of programmed cell death binding directly the proapoatotic proteins Bak and Bax (79). These mechanisms keep the cell alive as long as possible in order to permit the virus replication. The E2 gene products (E2A and E2B) are proteins that are necessary for the replication of viral genome and the ensuring transcription of late genes. The latters are a DNA polymerase, the preterminal protein (pTP) and the 72-kDa single stranded DNA binding protein (DBP). The E3 gene expression is indispensable for subverting the host defence mechanism, allowing the persistence of infected cells. Indeed, the E3-gp19K can interfere with the presentation of the viral antigen, preventing the translocation of MHC class I (major histocompatibily complex) molecules to the cell surface by sequestering them in the endoplasmic reticulum (80). Moreover, the E3-10.4K, 14.5K and 14.7K proteins inhibit the apoptotic pathway inducing the clearance of TNF-α, Fas ligand (FasL) and TRAIL receptors from the cell membrane. The gene products derived from the E4 cassette are involved in cell cycle control (E4orf6 cooperates with the E1B-55K protein in the sequestration of p53), promote virus replication and shut-off the host protein synthesis (81). During the last steps of early phase of the adenovirus infection, the viral DNA replication begins but requires sequences within the ITRs as origin of replication. Moreover, because the

viral genome does not have telomeres, the integrity of DNA ends is ensured by the viral protein pTP. This protein is covalently linked to the 5' end of each genome strand and acts as a primer for the viral DNA polymerase. The genes are encoded on both strands of DNA in a series of overlapping transcription units.

1.8.2 Late gene expression and viral assembly

After viral DNA replication, transcription of late genes begins. A key role in the control of this phase is played by the major late promoter (MLP), which is attenuated during the early stage of infection. In fact, during the "early phase", the basal level of transcription is low while, after the viral DNA replication and the high expression of IVa2 and IX genes, the transcription via the MLP is fully functional. From the MLP, 5 genes (L1-L5) are transcribed as single pre-mRNAs, each one encoding from 15 to 20 different mRNAs by differential splicing and polyadenylation. These transcripts encode structural proteins and other proteins involved in virion assembly. The virion assembly takes place in the nucleus, but the hexon trimerization begins in the cytoplasm and, subsequently, the hexon trimers move to the nucleus where they are associated with pentons and minor proteins to form the capsid (82). The viral genome encapsidation requires the L1-52/55K, IVa2, L4-33K proteins (83-85) and the packaging signal, which consists

in a series of seven repeats (A1-A7), enriched in AT, at the left end of the adenoviral DNA . These events are accompanied by changes in the nuclear structure. About 30 hours after infection, the host cell is lysed in a process involving the ADP protein (adenovirus death protein), a product of E3 gene, which is expressed only during the late phase of infection and is transcribed from MLP rather than E3 promoter (86).

1.9 Adenoviral vectors

Adenoviral vectors can be classified into first, second and third generation adenoviral vectors.

To date, third generation adenoviral vectors (commonly named helper dependent adenoviral, HD-Ad vectors) are the most successfully devices used for systemic gene therapy since their safety profile is strongly superior if compared to first and second generation adenoviral vectors.

First generation (FG-Ad) vectors are made by removing the E1 and/or E3 genes cassette. This genetic modification impairs the ability of virions to replicate and for this reason FG-Ad vectors are defined "*replication-deficient adenoviral vectors, RDA"*) **(Figure 8)**.

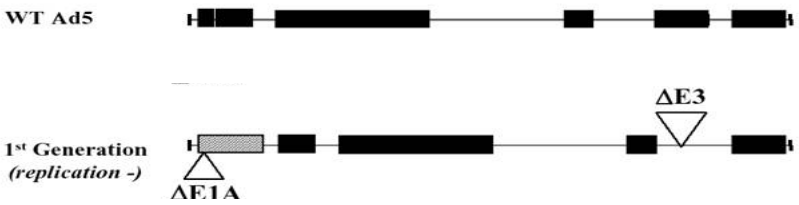

Figure 8: FG-Ad vectors. FG-Ad vectors derive from the deletion of E1 and E3 regions of the adenoviral backbone (white triangles). The structure of the wt adenovirus is reported for comparision.

These vectors retain the ITRs, the packaging signal and the other genes whereas the E1/E3 cassettes are replaced by a transgene of 6-8 kb long, often under the control of a heterologous promoter. The production strategy of FG-Ad vectors consists in the generation of the adenoviral genome by homologous recombination between a backbone plasmid (pAdEasy), expressing all adenovirus genes except E1 and/or E3, and a plasmid shuttling the gene of interest.

When the vector genome is cloned, its large scale production is made by transfecting the HEK-293 cell line, a human embryonic kidney-derived cell line, that provide the E1 functions *in trans* (87) **(Figure 9)**.

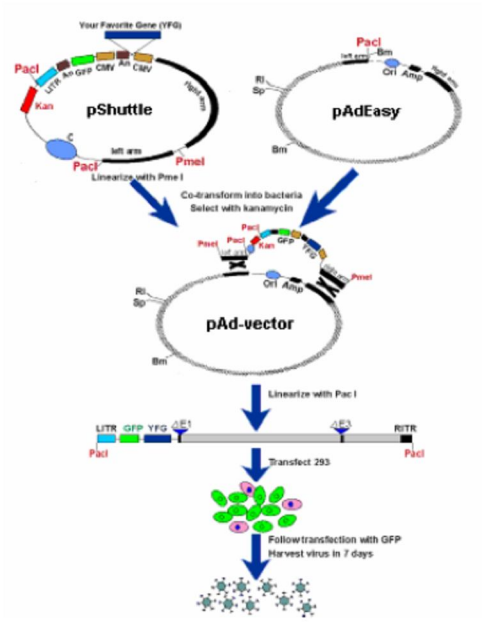

Figure 9: FG-Ad vectors production. A plasmid expressing the transgene of interest (pShuttle) is recombinated with a backbone plasmid (pAdEasy), expressing all adenovirus genes except E1 and/or E3. After the homologous recombination, the pAd vector is linearized and tranfected in 293 cells to proceed with the large scale production of vector.

Although FG-Ad vectors exhibit many advantages, as the ability to infect differentiated cells, liver tropism after systemic administration and high titer production ($1x10^{13}$ vp/ml), some drawbacks are still present. The first is the possible recombination between the E1 region sequences in the packaging cells (HEK-293) and the recombinant virus during its rescue. This recombination event can generate a viral progeny with functional E1 genes that becomes replication

competent adenovirus (RCA). Despite this inconvenient, a second and more troublesome problem associated with the use of FG-Ad vectors consists in their stimulation of the host immune response. This response is due to low levels of vector replication, that can occur even in the absence of the E1 genes (88), resulting in the destruction of transduced cells and in the low persistence of transgene.

In order to prevent these problems, second generation (SG-Ad) vectors have been proposed. These vectors are characterised by deletion of E2 and/or E4 coding sequences, providing both the benefits of a less probability of recombination to give RCA and a larger capacity for the transgene insertion **(Figure 10)**.

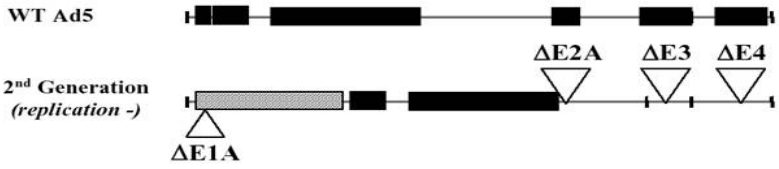

Figure 10: SG-Ad vectors. SG-Ad vectors derive from the deletion of E1, E2, E3, E4 regions of the adenoviral backbone (white triangles). The structure of the wt adenovirus is reported for comparision.

Nevertheless, the inhibition of viral gene expression by E1 gene is not much efficient. For this reason, the host immune response is a major impediment in using these vectors for applications requiring long-term gene expression.

Third generation, helper dependent adenoviral (HD-Ad) vectors are the product of the complete deletion of adenoviral wild type backbone, since they lack of both early and late genes and present only the ITRs and packaging signal of the wt adenovirus backbone **(Figure 11)**.

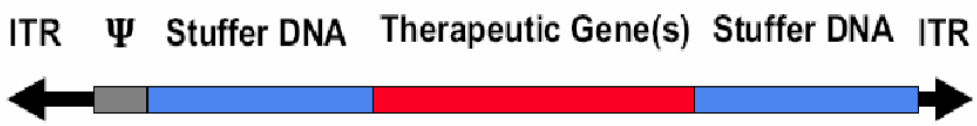

Figure 11: HD-Ad vectors. HD-Ad vectors derive from the deletion of all regions of the adenoviral backbone that are substituted with stuffer DNA (blue) and the expression cassette (red). The viral ITRs and the packaging signal (Ψ) are the only sequence of the wt adenoviral backbone that are still present in the construct (in black and grey respectively).

As a result they have low toxicity, very high capacity, and do not elicit immunological responses against the vector, thus allowing prolonged transgene expression (59,60).

CHAPTER 2

MATERIALS AND METHODS

2. MATERIALS AND METHODS

The research presented in this thesis required the use of many experimental methods. They are described in this chapter in detail.

2.1 E.Coli XL10-Gold and BL21 competent cells production and transformation

Rubidium chloride method for transformation competent cells

Medium: LB broth

TfbI, pH 5.8 with dilute acetic acid

Potassium acetate	30 mM
Rubidium chloride	100 mM
Calcium chloride	10 mM
Manganese chloride	50 mM
Glycerol	15% (v/v)

TfbII, pH 6.5 with dilute NaOH

MOPS	10 mM
Calcium chloride	75 mM
Rubidium chloride	10 mM
Glycerol	15% (v/v)

2 ml of an overnight culture of tetracycline/chloramphenicol resistant XL10-Gold (Stratagene, CA, U.S.A) or BL21 (Stratagene, CA, U.S.A) was inoculated into 200 ml LB broth (AppliChem, GmbH). Incubation at 37°C was performed with aeration to an adsorption of A550 = 0.48. Then the suspension was kept on ice for 15 minutes. After that, the bacterial cells were aliquoted into 50ml Falcon tubes and pelleted at 3000 rpm for 5 min at 4°C. The supernatant was discarded, cells were resuspended in 20 ml TfbI (0.4V of the original volume) and iced for 15 minutes. Cells were again centrifuged at 3000rpm for 15 min at 4°C, then resuspended in 2 ml per Falcon tube of TfbII (0.04V of the original volume) and kept on ice for 15 min. For storage, cells were aliquoted in microfuge tubes (50μl each), quick-frozen in a dry ice/ethanol bath and kept at -80°C. Competent XL10-Gold or BL21 cells were thawed on ice for 3 minutes, mixed by gentle tapping and briefly centrifuged at 3000rpm in a tabletop centrifuge. They were then resuspended by gentle pipetting, added to pre-chilled DNA and mixed either by tapping or gentle pipetting. A 30 minute incubation on ice after that was followed by a 45 seconds heat shock at 42°C with gentle tapping once after 45 sec. Cells were then put directly on ice for 2 minutes. 0.5 ml of LB medium was added and the transformation reaction was kept in a shaker (300rpm) at 37°C for 45 minutes. Following that, the volume was reduced by centrifugation and discarding of the supernatant to 150-200 μl. Cells were then plated with a sterile glass spreader on pre-warmed LB-agar plates containing the respective

antibiotic. If β-Galactosidase activity was used a selection marker, 40 μl of X-Gal solution (AppliChem, GmbH) was added before plating. Plates were dried for 10 minutes with an open lid at 37°C and then incubated overnight.

2.2 Construction of hPAH expression plasmid and site-directed mutagenesis

PAH wt and mutant constructs were obtained by modifying the plasmid pMAL Xa PAH, kindly provided by P. Waters (McGill University-Montreal Children's Hospital Research Institute, Montreal, Canada) in order to digest the fusion protein MBP-hPAH with enterokinase. The plasmid was modified by introducing the enterokinase site downstream the sequence encoding the factor Xa site by site directed mutagenesis using the primers:

5'GATGACGATGACAAGTCTACTGCGGTCCTGG3'

3'GCCCTAACTCCCTTCCCTACTGCTACTGTTC5'

and Quick Site directed mutagenesis kit (Stratagene, CA, U.S.A). Subsequently, each mutation was introduced into pMAL Xa Ek PAH using mutagenic primers and Quick Site directed mutagenesis kit (Stratagene, CA, U.S.A) (Table 1). The modified plasmid and the resulting clones were sequenced to verify the introduction of each single mutation.

Mutation	Mutagenic primer 5’	Mutagenic primer 3’
pN223Y	catgaagattacattccccagctggaagac	gtcttccagctggggaatgtaatcttcatg
pR297L	tgttttcagatctcagctttgcccagtttt	aaaactgggcaaagctgagatctgaaaaca
pF382L	actgtcacggagttgcagcccctgtattac	gtaatacaggggctgcaactccgtgacagt
pK398N	gccaaggagaacgtaaggaactttgctgcc	ggcagcaaagttccttacgttctccttggc
pQ419R	acccatacacccgaaggattgaggtcttgg	ccaagacctcaatccttcgggtgtatgggt
pQ301P	cgcagctttgccccgttttcccaggaaatt	aatttcctgggaaaacggggcaaagctgcg
pI65M	acctgacccacatggaatctagaccttctc	gagaaggtctagattccatgtgggtcaggt

Table 1 List of the oligonucleotide primers used for site-directed mutagenesis.

2.3 Expression and purification of hPAH in E.Coli

Expression plasmids were transformed into BL21 cells and the colonies were selected using LB plates with ampicillin (0.1 mg/ml, AppliChem, GmbH). Bacteria were grown to 2 x 10^{8} cells/ml (A_{600} ~0.5) and overexpression of wild-type and variant MBP-PAH fusion proteins was induced with 1 mM isopropylthio-b-D-galactoside (IPTG, AppliChem, GmbH) for 16 hours. Cells were harvested by centrifugation and treated according to the instruction manual of pMAL protein fusion and purification system (New England Biolabs, MA, U.S.A.). The fusion protein was digested on and at room temperature with Enterokinase to obtain wt and mutant forms of PAH without MBP tag (New England Biolabs, MA, U.S.A.),

using 0.5 ng of enzyme for every 50 µg fusion protein. The mixture was then applied to a hydroxyapatite (Bio-Rad Laboratories, CA, U.S.A.) column (1 cm x 10 cm) to remove maltose. MBP was isolated from the cleavage mixture by re-binding to amylose resin and the tetrameric fusion protein was then collected by size-exclusion chromatography with a HiLoad 16/60 Superdex 200 column (GE Healthcare, U.K.). Protein concentrations were determined spectrophotometrically with the use of the absorption coefficient A280 or the dye-binding Bradford assay (Bio-Rad Laboratories, CA, U.S.A).

2.4 Assay of PAH activity (purified proteins)

For each wt and mutant form of PAH, the activity was assayed at 25 °C, as previously described (11). Briefly, 50 µl of standard reaction mixture contained 0.1 M Na-Hepes, pH 7.0, 1 mg/ml of catalase, 100 mM ferrous ammonium sulphate, 5 mM DTT, 1 mM L-Phe, [^{14}C] L-Phe (Amersham, Buckinghamshire, UK), and 75 mM (6R)-tetrahydrobiopterin (BH4, Sigma-Aldrich, U.S.A). The enzyme (1-4, µg of hPAH) was preincubated for 2 min at 25° C in a mixture containing buffer, L-Phe and catalase. Then, Fe (II) was added and allowed to incubate for 1 min with the enzyme. The reaction was started by the addition of BH4 and DTT, and after 1 min was stopped by boiling. After centrifugation at room temperature and maximum speed, a 16 µl aliquot of supernatant was applied on a thin−layer chromatography (TLC, Polygram SIL N-HR/UV$_{254}$ Macherey-

Nagel, GmbH) system and the amount of ^{14}C radiolabeled L-Phe converted to L-Tyr was measured; the mean PAH activities were calculated from the three sets of protein preparations. The residual activities of mutant PAH enzymes were expressed as a percentage of wild type enzyme activity.

2.5 Electrophoresis and immunoblotting

SDS/PAGE was performed at 100 V (2 h) in a 10% (w/v) polyacrylamide gel; the purification of all proteins was verified after staining with Colloidal Comassie (Pierce, U.S.A.). The absence of MBP contamination in all preparations was determined by western blot analyses. Immunoblotting was performed using affinity-purified rabbit anti-human PAH (11) and mouse anti- MBP (New England Biolabs, MA, U.S.A.) as primary antibodies. The enhanced chemiluminescence (ECL) (Amersham, U.K.) was used for the immunodetection.

2.6 Generation and characterization of the HD-Ad vector

hPAH cDNA was excised from the expression vector pcDNA3−PAH, kindly provided by Paula Waters, cloned into pGEM (Invitrogen, CA, U.S.A) and cut by NotI digestion (New England Biolabs, MA, U.S.A). It was then ligated with a NotI plasmid containing the PEPCK promoter, a fragment of the human ApoA−1 intron and the bovine growth hormone polyadenylation signal. The expression cassette was excised from this plasmid by AscI digestion and cloned into pΔ28, a plasmid containing the viral Ad ITRs (left ITR and packaging signals: 1−440 bp; right ITR: 35,535-35,935 bp, accession n.NC001406), the packaging signal and human stuffer DNA (the 15,730-26,835 BamHI fragment of the C346 cosmid, accession n.:L3948, and the 1799-17853 EclXI/PmeI fragment from the HPRTB gene, accession n.:HUMHPRTB), obtaining pΔ28PEPCK PAH.

A pΔ28 carring the GFP sequence under the control of the CMV promoter was also constructed to follow the *in vitro* amplification of the vector.

The identity of both recombinant HD plasmids was confirmed by restriction enzyme digestion.

HD-Ad DNA was released from pΔ28PEPCKPAH and pΔ28CMVGFP plasmids by digestion with PmeI (New England Biolabs, MA, U.S.A.) and produced according to the protocol described by Palmer and Ng with some modifications

aimed to rescue a higher amount of viral vector. The viral vector was then purified by two CsCl (Roche Diagnostic, GmbH) step gradients and the HD-Ad band was collected and dialyzed. The virus suspension was taken out of the dialysis cassette (Pierce, U.S.A.) and 100 µl aliquots were stored at −80°C. The vector was quantified by OD260 determination.

For structural characterization, DNA digested with KpnI (New England Biolabs, MA, U.S.A.) was run on an ethidium bromide – stained 1% agarose gel. For comparison, the parental plasmid was digested with PmeI in addition to the enzyme just named. For determination of helper contamination, DNA digested with PstI (New England Biolabs, MA, U.S.A) was transferred to a nylon membrane for Southern hybridization analysis (Hybond, Amersham Pharmacia Biotech). The [a-32P] dCTP random prime-labeled adenoviral packaging signal probe was used to distinguish between the 1.6-kb vector-specific and the 1.0-kb helper-specific bands. Helper contamination was also assessed by real time PCR, using the following primers: H1 FW: TGTGGGCCATATTTTTTGGG e H1 RW: CAGGCGAGCTTGTGTGGAG. The reaction was performed under the following conditions: at 50°C for 2 min and 95°C for 10 min, followed by 40 cycles of 95°C for 30 sec and 68°C for 30 sec.

2.7 Mouse injection and sample collection

Breeding pairs of BTBR-*Pahenu2* mice were purchased from The Jackson Laboratory (Bar Harbor, ME, USA). A colony was maintained by mating heterozygote females with homozygous males in the Animal House at Ce.In.Ge, Biotecnologie Avanzate, Naples, to obtain sufficient numbers of Pahenu2 homozygote mice for this study. Homozygous mice are distinguished from their heterozygous littermates by their lighter coat colour. The genotype was confirmed by restriction fragment length polymorphism analysis. The Pahenu2 mutation creates a new Alw26I restriction site in exon 7. Genomic DNA was extracted from tail samples and exon 7 of the PAH gene was amplified using primers in introns 6 and 7 with Taq polymerase (Applied Biosystem, U.S.A). The resulting PCR product was then overnight digested with Alw26I (Fermentas, U.S.A). The restriction fragments were separated by electrophoresis on a 2% agarose gel at 90 V for 2 h.

Mice were housed in groups (n=4-5) in standard cages (29x17.5x12.5 cm) at a constant temperature (22±1°C) and maintained on a 12 h light/dark cycle. They had unlimited access to water and a diet containing 18.0% protein without L-Phe restriction (4RFU, Mucedola s.r.l, Italy) throughout the whole experimental period. Three-week-old mice were injected with $1x10^{14}$ viral particles of HD-Ad-PAH/kg into the tail vein. Blood samples were collected at various time points.

The liver, kidney, heart, and lungs were isolated from each HD-Ad injected Pahenu2 mice for analysis.

Experiments were conducted in conformity with protocols approved by the veterinary department of the Italian Ministry of Health and in accordance with the ethical and safety rules and guidelines for the use of animals in biomedical research provided by the relevant Italian laws and European Union directives (n. 86/609/EC). All efforts were made to minimize the animals' suffering. All mice subjected to behavioural tasks were gently handled 5 min/d for 2 weeks before the experiments.

2.8 Plasma Phe and Tyr tandem mass spectrometry determination

Dried serum spots on filter paper were prepared by punching out a circle with a diameter of 3 mm. A total of 200 µl of MeOH containing internal labelled standards were added. The mixed contents were allowed to stand for 20 min at room temperature. The supernatant was transferred to an eppendorf, evaporated to dryness under nitrogen, and incubated with 80 µl of Butanol-HCl 3N at 65°C for 25 min. The solvent was evaporated under nitrogen and the derivatized sample will be reconstituted in 300 µl of water-acetonitrile + 0.1% formic acid 50:50 solution before injection in the API 2000 LC/MS/MS system.

2.9 Assay of PAH activity (eukariotic cell extracts)

PAH enzyme activity assay was performed on the cytoplasmatic extracts of 116 cells, infected with the HDAd-hPAH vector and collected two days after the transduction. The assay was conduced in a final volume of l00 µl containing 10mM Tris HCl pH 7.4, 25 mM L-Phe, [^{14}C] L-Phe, catalase, 100 µg of total protein extract and a BH4 solution containing DTT. The reaction was started by adding BH4−DTT, incubated at 25°C o.n., stopped by boiling for 5 min and centrifuged at room temperature and maximum speed. A 16 µl aliquote of supernatant was applied on a thin−layer chromatography system and run for about 3 hours at room temperature in CHCl3−CH3OH−NH4OH−H20 (55:35:10 vol/vol). Each amino acid spot was cut out, placed in a scintillation vial with liquid scintillant and measured for [^{14}C] L-Phe and converted [^{14}C] L-Tyr.

-

2.10 Detection of HD-Ad DNA in tissues by Real Time PCR

DNA was isolated from mouse organs by a proteinase K digestion/phenol extraction/ethanol precipitation method. The HD-Ad viral genomic DNA was detected by Real Time PCR using the primers: Δ28 FW: GGTGTCGATCCATACCCGC e Δ28 RW: GAGGGATAAGCATGGGCTGAC.

The reaction was performed under the following conditions: at 50°C for 2 min and 95°C for 10 min, followed by 40 cycles of 95°C for 30 sec and 68°C for 30 sec.

2.11 Behavioral tasks

Two different tasks were used to assess the performances of PKU mice. The first and less invasive was the Morris water maze test. It was performed similarly to that described by Tang et al (89). The apparatus consisted of a circular pool (100 cm in diameter), surrounded by three-dimensional visual cues, containing opaque water at 21±1°C with a platform (8 cm in diameter) submerged 1 cm beneath the water surface. The training phase consisted of two sessions per day (3 h interval between sessions) over a 5 d period. Each session was composed of four trials with an inter-trial interval of ~5 min. The time to reach the target was measured. A probe test was performed after training, 24 h after the last session (to evaluate time-dependent memory retention of mice), in which animals were allowed to swim for 60 s in the absence of the platform. The percentage of time spent in each quadrant was recorded. A computerized video tracking system (Videotrack; Viewpoint) was used to collect data during learning phase and probe test. In the learning phase, the measure of the escape latency was used as dependent variable, and data were examined using two-way ANOVA with repeated measures. Data obtained in the probe trials were analyzed by Fischer's *post hoc* comparison, to

evaluate the spatial preference of each experimental group for each quadrant. Moreover, Student's *t* test was used to determine genotype effect on the spatial preference.

The Fear Conditioning was performed according to Shumyatsky et al. (90). Mice were individually placed in a conditioning shock chamber (Freeze Monitor; San Diego Instrument). Conditioning was assessed 24 and 27 h after training by scoring freezing behavior, defined as the complete lack of movement. Contextual fear conditioning was evaluated and analyzed for 3 min in the context in which mice were trained, instead cued fear conditioning was assessed by masking the training context and subjecting mice to the cue (a 85 decibel sound). Both training and testing sessions were videotaped. Student's *t* test was used to determine genotype effect on the freezing behavior, expressed as percentage of time spent in freezing. A significance level of $p < 0.05$ was accepted as statistically significant in all the experiments performed. All measures are expressed as mean ± SEM. All statistical analyses were performed with StatView software (version 5.0.1.0; SAS Institute).

2.12 Electrophysiological studies

All animals were studied using standard *in vitro* electrophysiological recordings. Preparation of hippocampal slices was performed in accordance with the European Communities Council Directive (86/609/EEC). Vibratome-cut

parasagittal slices (400 μm) were prepared, incubated for one hour and then transferred to a recording chamber submerged in a continuously flowing artificial cerebrospinal fluid (30°C, 2-3 ml/min) gassed with 95% O2- 5% CO2. The composition of the control solution was (in mM): 126 NaCl, 2.5 KCl, 1.2 MgCl2, 1.2 NaH2PO4, 2.4 CaCl2, 11 Glucose, 25 NaHCO3. Field excitatory postsynaptic potentials (fEPSPs) were recorded in the stratum radiatum of the CA1 using glass microelectrodes (1–5MΩ) filled with aCSF. Synaptic responses were evoked by stimulation of the Schaffer collateral/commissural pathway with a concentric bipolar stimulating electrode. Data were expressed as mean ± SEM and assessed for significance using the Student's t test or ANOVA, as appropriate. A minimum of 6 animals per group was used for all electrophysiological recordings.

2.13 Expression of NMDA and AMPA receptor subunits by Western Blot

BTBR-Pahenu2 were killed, the hippocampus was dissected out and immediately frozen. It was then homogenated in a buffer containing 2% SDS, 50 mM Tris-HCl pH 6.8, 1 mM EDTA, 1mM NaF, 1 mM $NaVO_3$, 1x Complete Inhibitor (Roche Diagnostics, GmbH). Aliquots (2μl) of the homogenate were used for protein determination using a Bio-Rad Protein Assay kit. Equal amounts of total proteins (30μg) for each sample were loaded onto 10% polyacrylamide gels. Proteins were

separated by SDS-PAGE and transferred overnight to membranes (polyvinylidene difluoride) (GE Healthcare, U.K.).

The membranes were immunoblotted using selective antibodies against NR2B, (1:1000; Millipore, MA, U.S.A), NR2A (1:1000, Sigma-Aldrich, U.S.A.), Glu1 (1:1000, Sigma-Aldrich, U.S.A), Glu2/3 (1:1000, Sigma-Aldrich, U.S.A), and GAPDH (1:6000; Santa Cruz, CA, U.S.A.). Blots were then incubated in horseradish peroxidase conjugated secondary antibodies, and target proteins were visualized by ECL detection (GE Healthcare, U.K.), followed by imaging using a Bio-Rad Chemidoc instrument with quantitation by Quantity One software. Optical density values were normalized to GAPDH for variations in loading and transfer. Normalized values were then averaged and used for statistical comparisons (Student's *t* test).

CHAPTER 3

RESULTS

CHAPTER 3- RESULTS

During my PhD, I treated two different aspects of PKU. The first regarded the characterization of new mutant forms of the PAH enzyme that were identified in Italian PKU patients.

The other aspect was the cure of the pathologic phenotype of PKU by means of a HD-Ad vector expressing PAH. I delivered the wild type PAH gene to the hepatic tissue of PKU mice that after the treatment showed a complete normalization of their pathologic biochemical features.

I also studied the behavioural profile of these mice to investigate if an early treatment with gene therapy could ameliorate their behavioural pathologic phenotype. These studies were integrated by electrophysiological analyses and by the determination of the expression levels of N-methyl-D-aspartic acid (NMDA) and α-amino-3-hydroxy-5-methyl-4-isoxazolepropionic acid (AMPA) receptor subunits that, as known, play a pivotal role in learning and memory processes and which were found to be imbalanced in PKU.

3. RESULTS

3.1 Mutagenesis and Expression in E.Coli of wild type and mutant forms of PAH

All the mutations analyzed have been previously expressed in human HEK293 cells using transient expression (10-12). As the amount of protein obtained in the eukaryotic system is not enough to consent a suitable purification and characterization of the molecular features of the PAH enzyme, recombinant proteins were produced in the prokaryotic system, using E.Coli BL21 cells.

The first step consisted in the introduction of the enterokinase site downstream the sequence encoding the factor Xa site in pMAL Xa PAH, in order to digest the fusion protein MBP-hPAH with enterokinase (**Figure 12**). In fact, it has been demonstrated that the cleavage of MBP-hPAH with factor Xa releases not only the full-lenght product but also a truncated form of the protein, lacking the 13 N-terminal residues, thus indicating that factor Xa digestion occurred also between the residues Arg- 13 and Lys-14 in the hPAH sequence. In this conditions, the recovery of full-length hPAH varied depending on the reaction temperature and time, as well as the protein:protease ratio (92). This problem is avoided when enterokinase is used. Indeed, the fusion protein MBP-Ek-hPAH is specifically cleaved by enterokinase at its target sequence (D4K) and only full-length hPAH

resulted from this cleavage. The introduction of the enterokinase site was done by site directed mutagenesis and confirmed by DNA sequencing. In the same way, all mutations were introduced into pMAL Xa Ek PAH and confirmed by sequence analysis.

After all the purification steps described in the *Materials and Methods section*, wild type and mutants PAH pure proteins were obtained in proper amounts (8-10 mg/liter of culture). An exception was represented by the Q301P mutant which showed a different behaviour and was recovered in lower amounts.

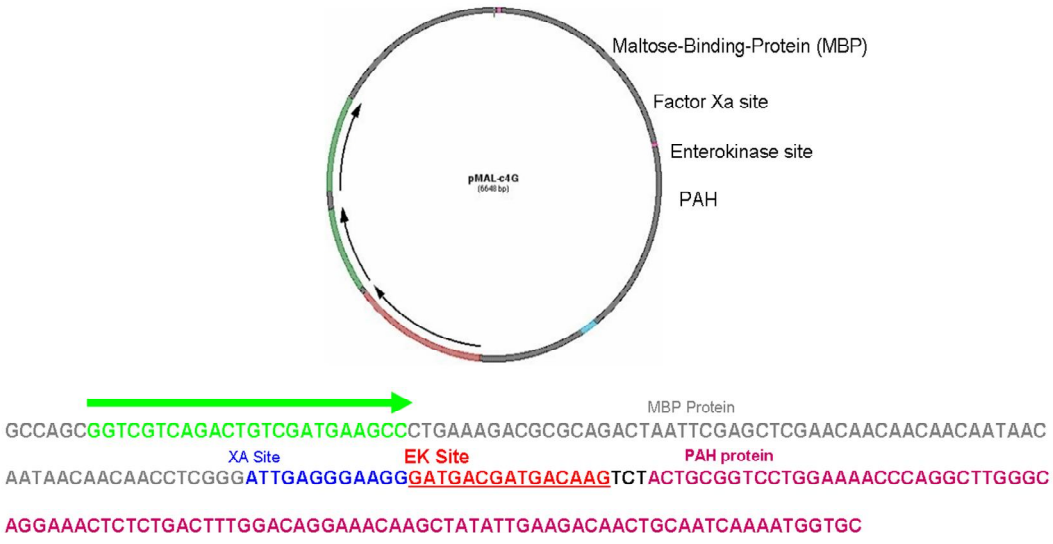

Figure 12: Schematic representation of pMAL Xa Ek PAH.The Xa and Ek sites are shown in blue and red respectively. The MBP and PAH gene are represented in grey and purple.

3.2 Electrophoresis and immunoblotting

The purity of all proteins was verified by SDS/PAGE followed by Colloidal Comassie staining. As shown in **Figure 13**, a band corresponding to the molecular weight of PAH monomer was present.

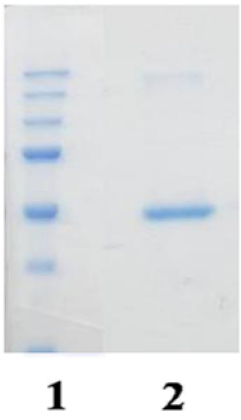

Figure 13: SDS PAGE analysis of purified hPAH by Colloidal Comassie staining. **Lane1** contains the protein stained marker; **Lane 2**: hPAH after the FPLC purification step.

The further confirmation that this band contained only PAH and not MBP was obtained by Western Blot. Immunoblotting performed using affinity-purified rabbit anti-human PAH and mouse anti- MBP showed that the purified protein did not contain any MBP trace, so confirming that the product was highly pure **(Figure 14).**

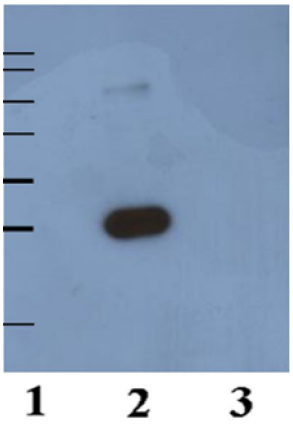

Figure 14: Western blot analysis performed on the hPAH wt protein. **Lane1** contains the protein stained marker. **Lane 2**: immunoblotting using anti-hPAH as primary antibody. **Lane 3** contains the same protein blotted with anti-MBP antibody.

3.3 Enzymatic activity analysis of wild type and mutant forms of PAH

PAH enzyme assay was performed after enterokinase digestion and purification of wt and mutant proteins. All mutants showed a residual lower activity compared to wt PAH. For all mutations, the enzyme activity measured in the prokaryotic system corresponded to those observed in human HEK293 cells (10-12).

3.4 Generation and characterization of the HD-Ad vector

A HD-Ad vector was constructed by inserting the human PAH-cDNA into the pΔ28 vector plasmid, as described in the *Materials and Methods section*. This vector, pΔ28-hPAH, contained the phosphoenolpyruvate carboxykinase (PEPCK) promoter, the apoA1 intron, the hPAH cDNA and the GH polyA signal **(Figure 15 A)**. The PEPCK promoter was inserted in the HD-Ad construct for its liver specificity in order to restrict the expression of the hPAH in the liver, the target tissue of the PKU disease.

After several passages of HD-Ad amplification in adhesion/suspension culture of 116 cells, the viral vector was rescued by CsCl gradient **(Figure 15 B)** and subjected to further studies to evaluate its structure and helper contamination.

As depicted in **Figure 15 C**, restriction digestion analysis of the vector and the parental plasmid DNA showed the expected bands and excluded gross vector rearrangements during rescue. Southern Blot analysis confirmed that the preparation was free of helper virus **(Figure 15 D)**. This result was further confirmed by real-time PCR that showed a 0.06% of helper contamination. The vector was then tested for its *in vitro* ability to express a functional PAH protein before the *in vivo* studies.

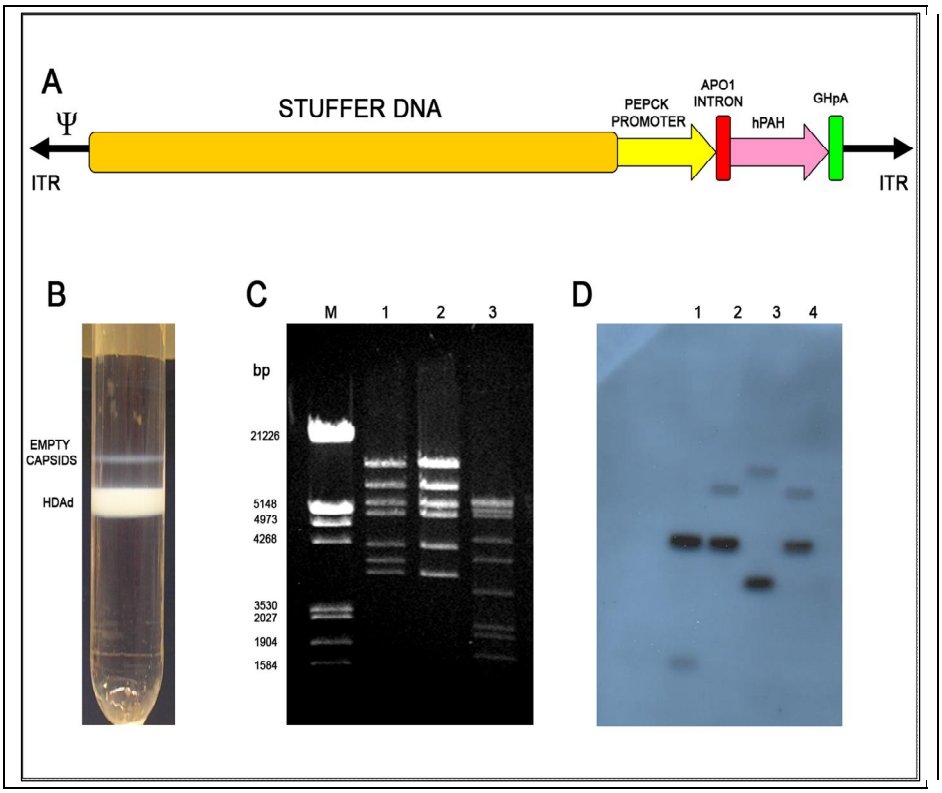

Figure 15: Structure and characterization of HDAd-hPAH vector. (a) Diagram of the vector used in this study: the HDAd-hPAH contains, in the pΔ28 backbone, the liver-restricted phosphoenolpyruvate carboxykinase (PEPCK) promoter, the human ApoAI intron, the hPAH cDNA and the human growth hormone poly A. **(b)** Purification of the vector by CsCl gradient following the final amplification of the vector in a suspension culture of 116 cells. The top band is of empty capsids, the more dense of HDAd-hPAH. **(c)** Restriction digests with Kpn1/Pme1 of parental plasmid (lane 1), HD-Ad hPAH (lane 2) and helper virus (lane 3) DNAs. The overlap between the structure of the plasmid and the viral vector indicates absence of gross vector rearrangements. **(d)** Analysis of helper virus contamination. The DNAs were digested and hybridized with the L-ITR plus the packaging signal sequence that give fragments of different length for the HDAd vector and the helper virus. Lane1: Pme1/Pst1 digested pΔ28 plasmid; Lane 2: Pme1/Pst1 digested pΔ28-PEPCK-hPAH plasmid; Lane 3: Pst1 digested Helper virus; Lane 4: Pst1 digested HDAd-hPAH.

A HD-Ad vector expressing GFP was used to monitor the amplification of the HD-Ad vector expressing PAH and was produced at the same time **(Figure 16)**.

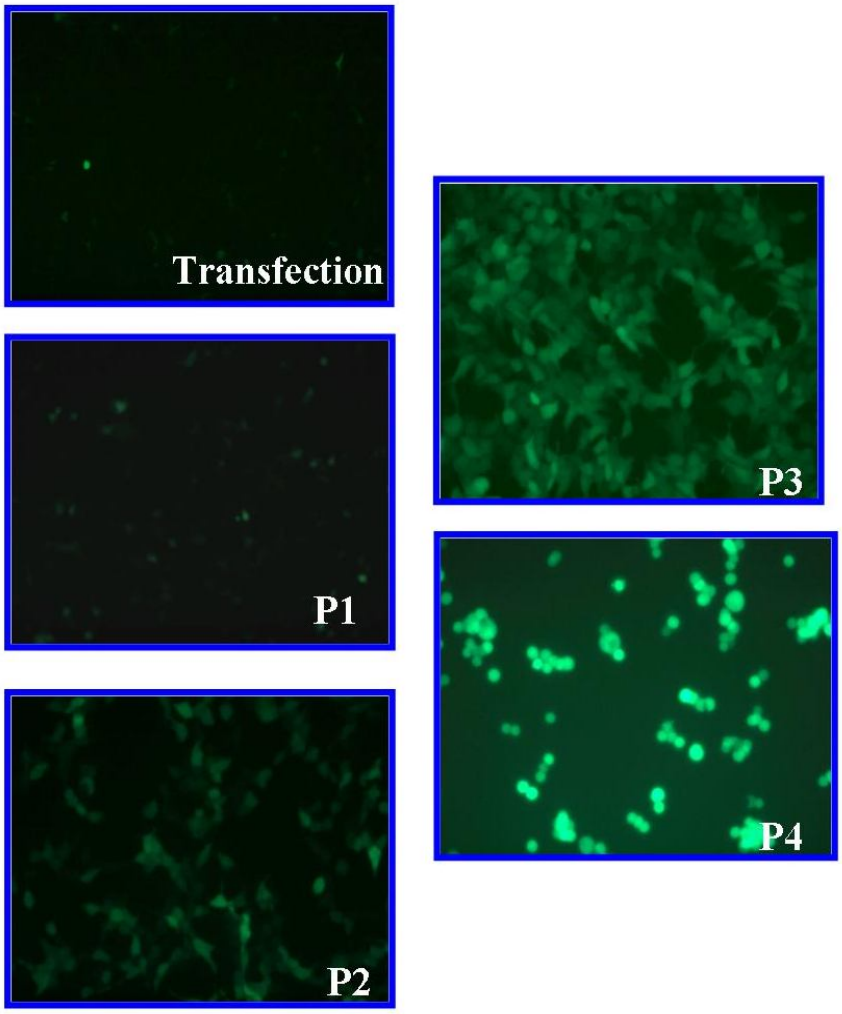

Figure 16: Amplification of a HDAd vector expressing GFP. Several passages (from transfection of the viral plasmid to suspension culture of infected cells) are showed. During each of these steps, the amount of viral vector expressing GFP rapidly increases.

3.5 Activity assay of HDAd-hPAH after in vivo transduction

116 cells were infected with the HDAd-hPAH vector and used for the *in vitro* assay, as described in the *Materials and Methods section*. Two days after the infection, HDAd-hPAH transduced cells were collected and cytoplasmatic proteins were isolated. Cells transduced with a control plasmid (pCDNA3-PAH) and untransduced cells were used as positive and negative controls respectively.

As shown in **Figure 17**, PAH activity was found both in the pCDNA3-PAH and HDAd-hPAH transduced cells but there was no expression in the untransduced cells. The lower signal for HD-Ad hPAH transduced cells could be explained on the basis of the liver specific promoter present in the viral construct.

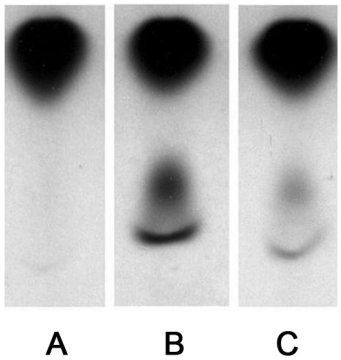

Figure 17: *in vitro* PAH activity assay by TLC. The PAH activity was assessed 48 hours after the transduction of 116 cells to evaluate the effectiveness of the viral construct in the expression and activity of hPAH. In the TLC system, Phe has a higher RF than Tyr. Assays were conduced in the presence of BH4 cofactor. Lane **A)** represents untransduced cells lane **B)** pCDNA3-PAH transduced cells and lane **C)** HDAd-hPAH transduced cells.

3.6 Effects of adenoviral treatment on hyperphenylalaninemia

Purified HD-Ad hPAH was used to treat 3-week-old BTBR PAHenu2 mice, by means of a single intravenous injection. To achieve phenotypic correction of PKU homozygous BTBR PAHenu2 mice, whose basal Phe and Tyr values were respectively 1200 μM and 25 μM , different doses of HD-Ad vector were tested, starting from $1x10^{13}$ viral particles (vp)/kg (n=3), increasing to $3x10^{13}$ vp/kg (n=3), and finally using a maximum dose of $1x10^{14}$ vp/kg (n=3) per animal. This pilot experiment allowed us to estabilish that serum Phe and Tyr levels were unchanged in mice treated with the lowest dose of the viral vector, whereas, mice treated with the intermediate dose reached the normal values (80 μM) in two weeks but increased four weeks after the treatment. Only mice treated with the highest dose obtained a normalization of Phe and Tyr two weeks and was stably maintained for all the observation period **(Figure 18 A,B)**. For this reason, $3x10^{12}$ vp were used for the successive studies.

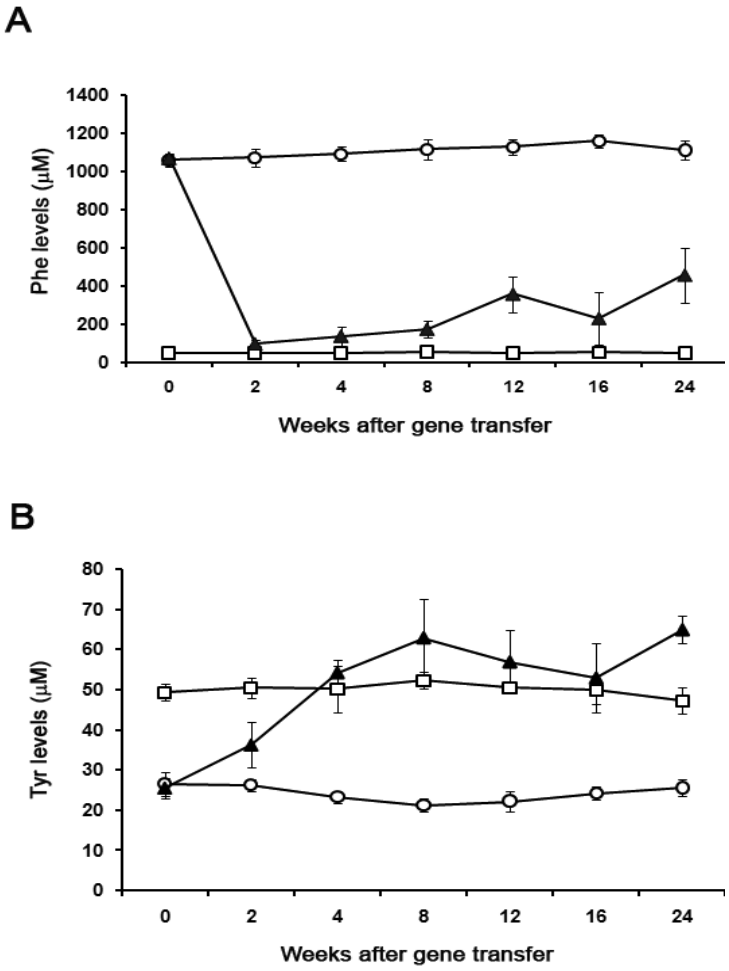

Figure 18: Time course of serum Phe and Tyr levels in PKU mice after intravenous administration of vector HDAd-hPAH. PKU mice (—○—) showed a severe hyperphenylalaninemia (Panel **A**) and a decrease of Tyr levels **(B)** before the treatment. This biochemical phenotype was rescued in HDAd-hPAH treated PKU mice (—▲—). Control mice were indicated as (—□—). Serum Phe and Tyr levels at various time points after HDAd-hPAH injection were compared with pre-injection levels using Student's *t*-test. Significant differences as compared to t = 0 found for all HDAd-hPAH treated animals were found at all time points.

Together with the normalization of Phe values, HD-Ad PAH treated mice showed a reversal of their hypopigmentation. In particular, visible changes started 1week after the injection of the viral vector and became complete 2 weeks after the treatment **(Figure 19 A,B)**. Treated homozygous BTBR PAHenu2 mice remained indistinguishable from wild-type and heterozygous mice over the whole experimental period.

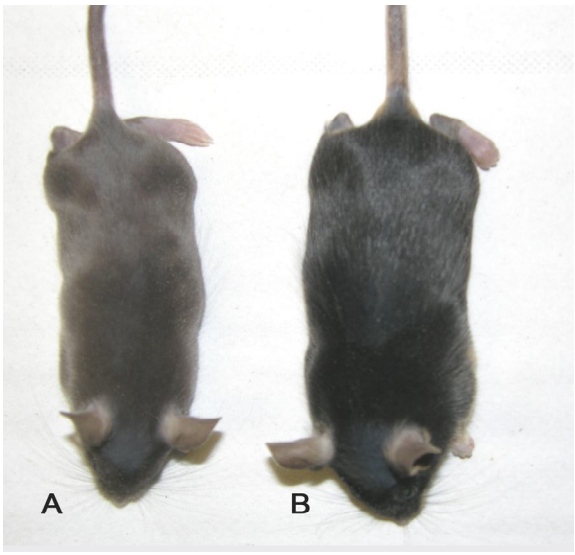

Figure 19: Coat color change in PKU mice after the administration of the vector. Owing to a reduction in serum Tyr, the precursor of melanin, PKU mice present a grey coat **(A)**. The characteristic hypopigmentation of PKU coat was completely reversed 2 weeks after the administration of the vector **(B).**

3.7 Effects of the adenoviral treatment on *in vivo* PAH enzymatic activity

A restoration of PAH enzymatic activity was observed 2 and 6 months after the administration of the vector in PKU mice **(Figure 20)**. PAH activities recovered to levels ranging from 15% to 20% of wild-type mice.

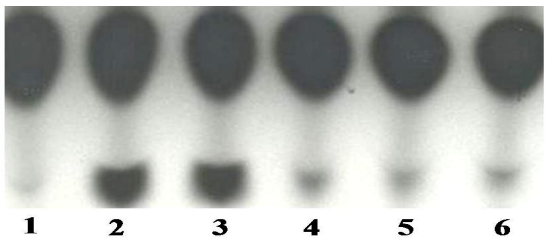

Figure 20: *in vivo* PAH activity assay by TLC. Levels of PAH enzyme activities were assessed in the liver of PKU HDAd-hPAH treated mice 6 months after the administration of the vector. Lane 1 shows untreated PKU mice, lanes 2-3 control mice, lanes 4-6 viral treated mice.

3.8 Detection of HDAd-hPAH DNA by Real Time PCR

Tissue distributions of recombinant adenovirus were examined in PKU mice. The amount of viral DNA was quantified by Real Time PCR. The majority of the recombinant virus was found in the liver. Viral DNA was also detected, in much lower quantities in the spleen, kidney, lung, heart and was undetectable in brain **(Figure 21).**

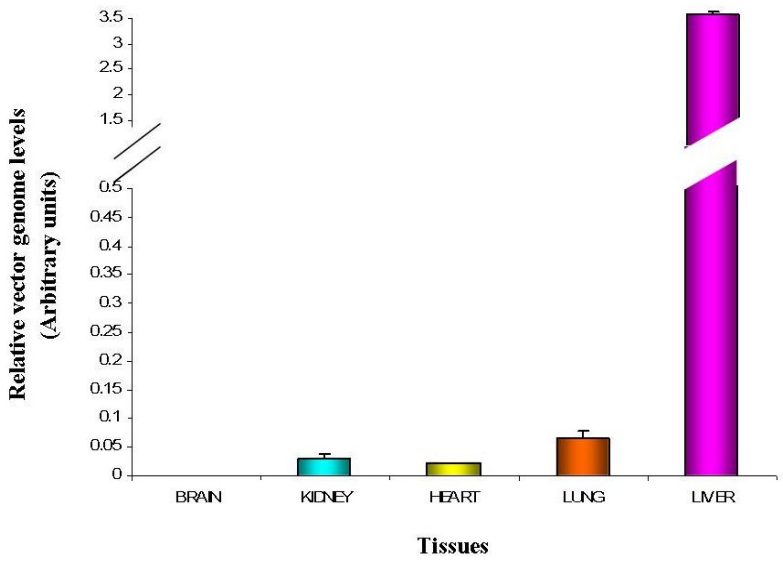

Figure 21: Detection of HD-Ad DNA in HDAd-hPAH tissue samples. The distribution of the viral vector was assessed by real time pcr in tissue samples taken from HDAd-hPAH treated mice. The HD vector DNA is particular abundant in the liver. Lung, heart, kidney are only marginally infected, instead in the brain the HD vector DNA is completely absent.

3.9 Behavioural tasks

It is established that NMDA receptors signalling plays a pivotal role in hippocampus related learning and memory. Thus, based on the evidence that Phe can inhibit the correct function of NMDA receptors, acting as an antagonist of the co-activator glycin (21,22), and supported also by other studies that showed behavioural deficits in the PKU mouse model, we assessed the performances of mice in two tasks: the Morris Water Maze and the Fear Conditioning.

The first experiments were performed with homozygous BTBR Pahenu2 mice and healthy controls, represented by heterozygous mice, that, as known, present normal levels of L-Phe.

We used only the Morris Water Maze was to explore the performances of HD-Ad treated PKU mice, since Fear conditioning was not a good task to evaluate the performances of these mice. In fact, freezing behaviour of both homozygous and heterozygous BTBR Pahenu2 mice was extremely reduced if compared to other strains (for example C57/BL6 mice), especially in the cue-version **(Figure 22 A,B).**

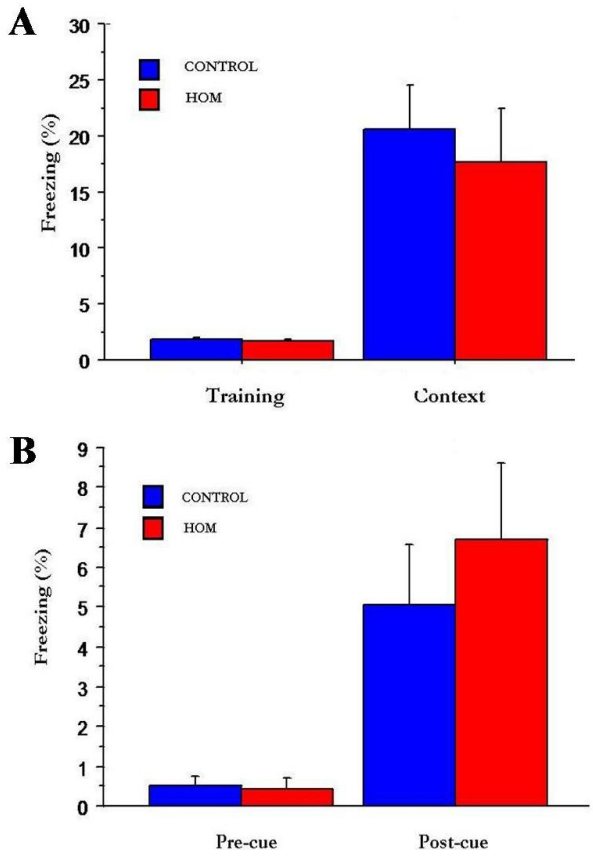

Figure 22: Fear conditioning of homozygous PKU (red bars) mice versus control (blue bars) mice. The performances of both groups of mice revealed a poor freezing behaviour.

The Morris Water Maze task was performed in two versions: a visible and a hidden platform version. The first was made to exclude any emotional, sensory and/or motor impairments in this animal model **(Figure 23 A)**. In the hidden version, on the other hand, PKU mice revealed a deficit in spatial learning that was recovered in HD-Ad treated PKU mice that showed a profile comparable to control, heterozygous mice **(Figure 23 B)**. This reflected also in the spatial memory profile, with a higher percentage of time spent in the goal quadrant for

HDAd-hPAH treated and heterozygous mice compared to PKU mice that did not display a particular quadrant preference **(Figure 23 C).**

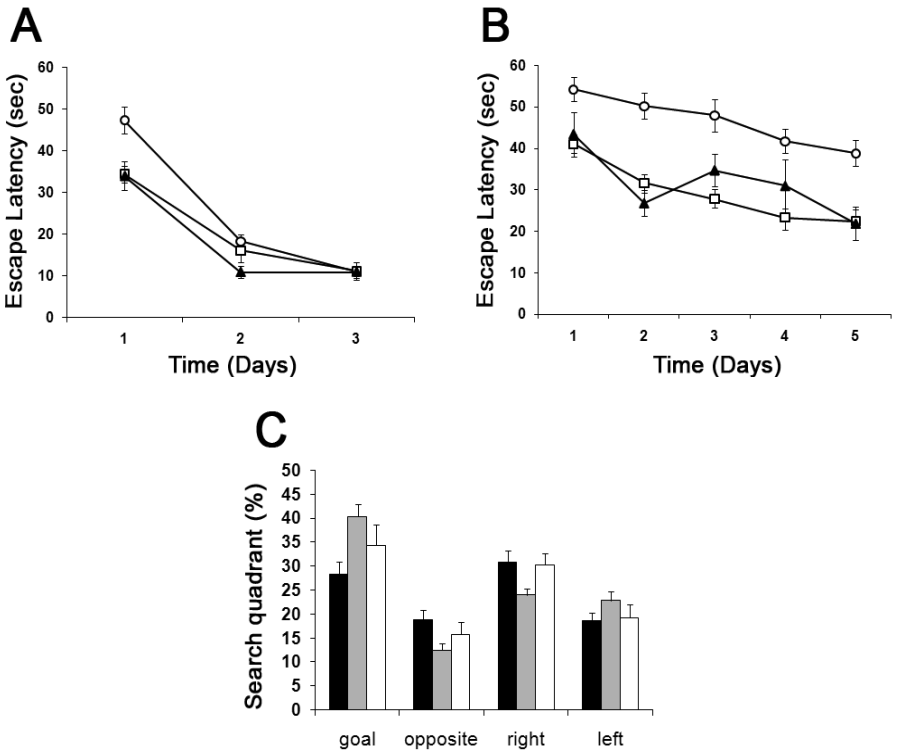

Figure 23: Correction of reference memory in 2 month-HDAd-hPAH treated mice. The Morris Water Maze task was used to evaluate reference memory impairments of PKU mice (—○—). The task was done in two versions (visible and hidden platform training). In the visible platform training, PKU mice displayed similar performances if compared to viral treated (—▲—) and control (—□—) littermates. In the hidden platform training, instead, PKU mice performed considerably worse than viral treated and control mice. Similar results were seen in the probe test, in which PKU mice (■, **C**) displayed deficits in spatial memory compared to control **(▩,C**) and viral treated mice **(□,C**).

The same effect was found in PKU mice that were treated for a longer period with the HDAd-hPAH vector **(Figure 24 A,B,C).**

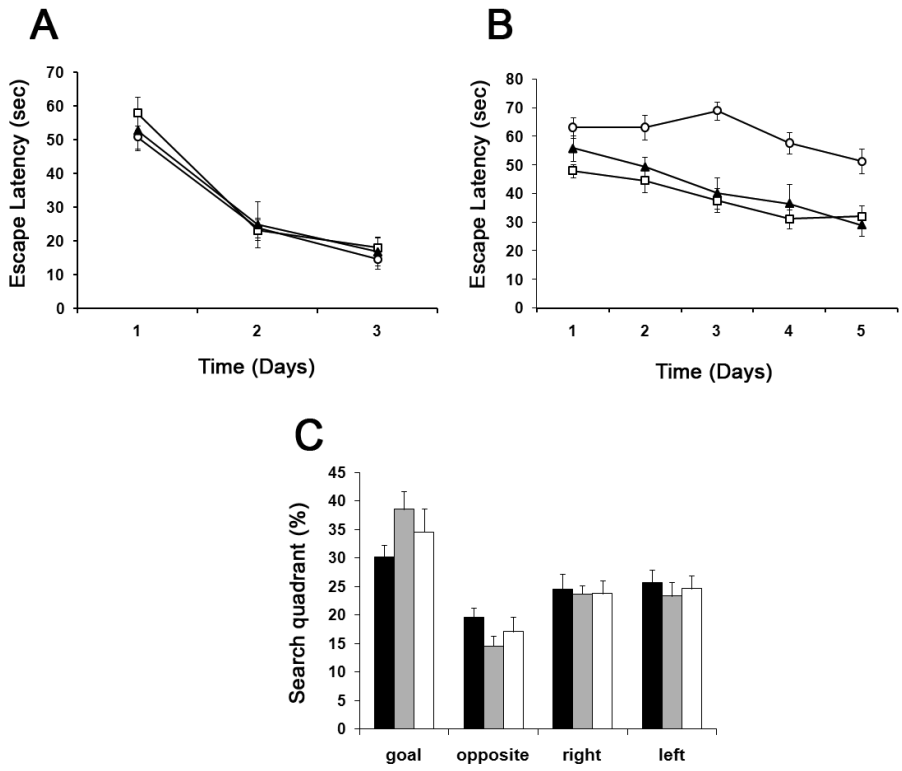

Figure 24: Correction of reference memory in 6 month-HDAd-hPAH treated mice. The Morris Water Maze task was repeated in another group of HDAd-hPAH injected mice, 6 months after the treatment, to confirm the benefic effect of the HDAd-hPAH vector in PKU mice. As for the 2 month-groups, untreated PKU mice displayed similar performances if compared to viral treated (—▲—) and control (—□—) mice **(A)** in the visible platform training, whereas they showed deficits in spatial learning (—○—, **B)** and memory **(■**, **C**) in the hidden version. HdAD-hPAH treated PKU mice, injected at 3 weeks of age, showed a rescue of the behavioral pathologic phenotype (—▲—,**B) (□,C**).

3.10 Electrophysiological studies

In order to verify if the memory deficits observed in homozygous PKU mice correlate with defects in synaptic plasticity, the electrophysiological phenotype of these mice in the Schaffer collateral pathway was explored by recording extracellular field potentials.

No significant difference in stimulus-response curves and in paired-pulse facilitation (PPF) between homozygous PKU and heterozygous control mice were found (data not shown), indicating that basal transmission was not affected by the mutation.

To determine whether synaptic plasticity might be altered in the same experimental groups, we studied long-term potentiation (LTP) induced by a high-frequency stimulation protocol (HFS). Stimulation at 100 Hz induced a severe deficit in LTP in brain slices from homozygous PKU mice compared to heterozygous control mice (50–60 min: heterozygous mice: 150% ± 10%; homozygous mice: 122% ± 10%, $p < 0.05$; **Figure 25 A**).

Starting from these data, we tested whether this deficit could be overcome by gene therapy and we found that LTP levels in HD-Ad treated mice were restored upon the treatment (50–60 min: viral, 141% ± 3%, $p < 0.05$; **Figure 25 B**).

Our results, summarized in **Figure 25 C,** indicate that gene therapy was able to reverse the deficit in synaptic plasticity observed in PKU mice.

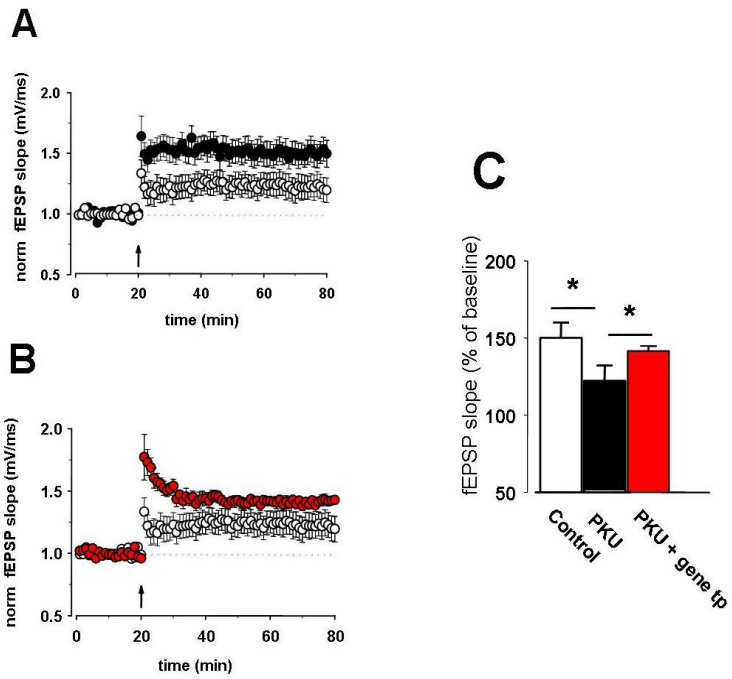

Figure 25: Effect of L-Phe on the modulation of hippocampal synaptic functions at CA1 synapses. A) Superimposed pooled data showing the normalized changes in field potential slope (±SEM) in homozygous PKU mice (white plots) vs heterozygous control mice (black plots) induced by HFS protocol. The degree of potentiation between 50-60 min after HFS was significantly lower in homozygous PKU (n = 7) compared to heterozygous (n = 6) mice. fEPSP slopes were recorded and were expressed as the percentage of the pretetanus baseline. A stimulation intensity that evoked 50% of maximal fEPSP response was used**. B)** Superimposed pooled data showing the effects of viral treatment on LTP in homozygous PKU mice (n = 8, red plots). **C)** Columns represent the average EPSP response measured between 50-60 min following HFS (asterisk indicates $p < 0.05$).

3.11 Expression of NMDA and AMPA receptor subunits by Western Blot

Expression analysis of NMDA receptor subunits in homozygous PKU mice showed an imbalance between NR2A and NR2B subunits, with an increased expression of NR2A subunit and a significant decreased expression of NR2B subunit.

On the other hand, western blot analysis of both GluR1 and GluR2/3 subunits of AMPA receptors revealed an up-regulation of GluR1 and GluR2/3 subunits that was particularly significant for GluR2/3.

As depicted in **Figure 26**, HDAd-hPAH treated mice presented a normalization of the expression of these subunits.

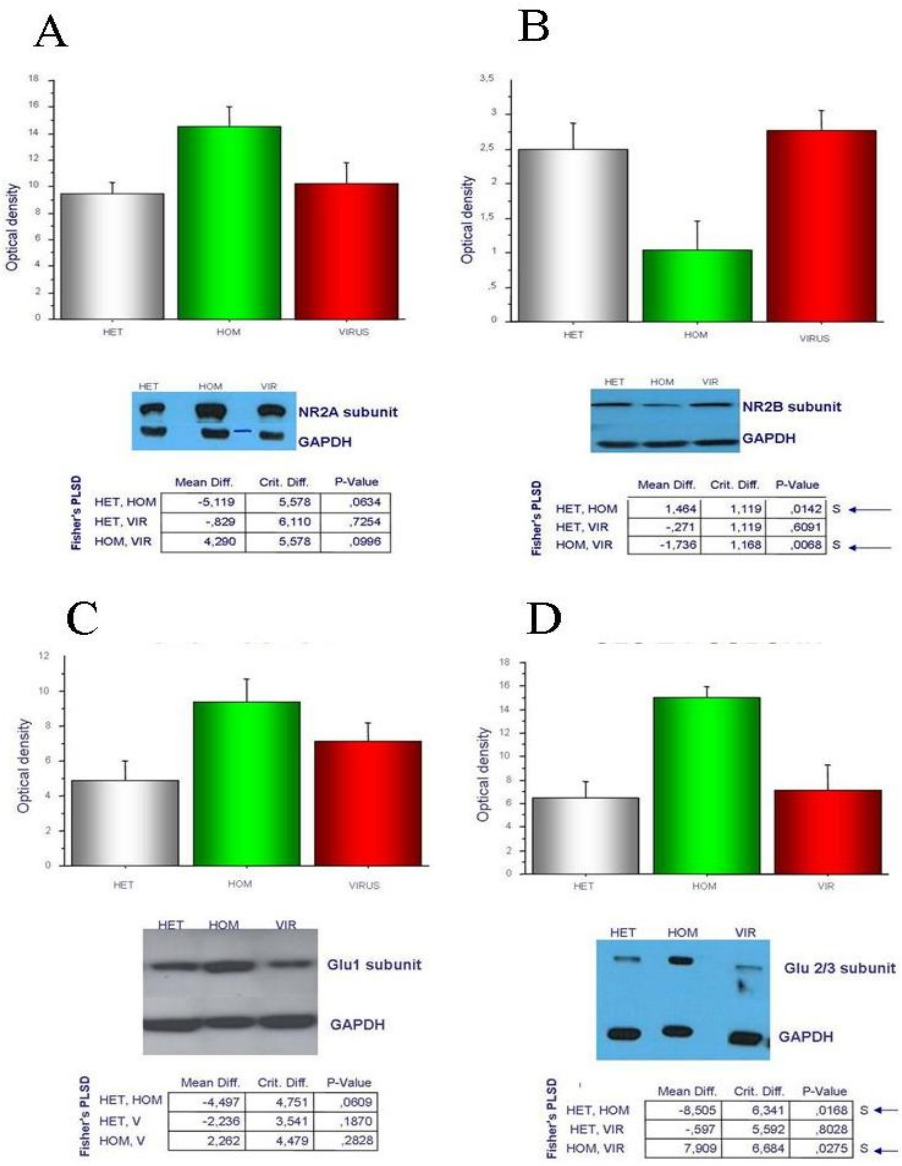

Figure 26: Expression analysis of NMDA and AMPA receptor subunits in HDAd-hPAH treated mice. Control mice are showed in grey, homozygous PKU mice in green and HDAd-hPAH treated mice are depicted in red. Panel **A** shows NR2A subunit, panel **B** NR2B, panel **C** Glu1 and panel **D** Glu2/3 subunit.

CHAPTER 4

DISCUSSION

4 DISCUSSION

Gene therapy for PKU patients could be a promising approach to prevent brain damage due to discontinuation of the arduous dietary restriction treatment. Several types of vectors, including retroviral, first generation adenoviral, and adeno-associated viral gene transfer vectors, have been examined for their potential to transduce liver, the prominent site of PAH expression and activity (51-56). In this context, adenovirus mediated gene therapy holds a significant potential thanks to the ability of adenoviral vectors to transduce the hepatic tissue. Nevertheless, the clinical translation of adenoviral gene replacement therapy for genetic disease is lagged by vector associated toxicity that is very significant for first and second generation adenoviral vectors (87). In fact, a previous attempt to cure PKU by means of a first generation adenoviral vector expressing PAH was successful but did not produce a long lasting effect due to the strong immune response that followed the administration of this type of adenoviral vector (51). Advances in vector production have led to the development of Helper-Dependent adenoviral vectors (HD-Ad) which are characterized by the deletion of all viral coding genes, so the chronic toxicity that follow their systemic administration is significantly reduced (59-60).

In this thesis, I have described a gene therapy approach based on a helper dependent adenoviral vector expressing PAH that was administered to 3-week-old PKU mice that, before the treatment, showed a severe hyperphenylalaninemia.

CHAPTER 4- DISCUSSION

Serum Phe levels were measured at different time points to follow the biochemical correction mediated by the therapeutic helper dependent adenoviral vector. The decrease in serum Phe levels was accompanied by an increase of Tyr levels that, as is known, is the precursor of neurotrasmitters and melanin. As a consequence, gene therapy treated mice started to change their grey coat color one week after the administration of the vector and became completely black two weeks after the treatment. By the way, the biochemical correction was only one of our objectives. In fact, we addressed our attention also on the effects of gene therapy on the neurological impairments of PKU mice.

It has been previously reported that PKU mice present behavioural deficits involving both spatial and non-spatial recognition that are not related to motor impairments or to high emotional reactivity to novelty (45).

Moreover, the authors that delivered the first generation adenoviral vector expressing PAH to PKU mice (52) noticed that gene therapy treated mice were more alert than their untreated counterparts, although they did not elucidate their phenotypic changes with behavioural studies. Later, other investigators (89) performed a behavioural characterization of gene therapy treated mice but they assessed only their locomotion and exploratory behaviour.

As the evaluation of the behavioural and neurological parameters in PKU mice after gene therapy could provide important experimental evidences for the efficacy of the proposed treatment, we deeply investigated the performances of

PKU mice. At this aim, we used the Morris Water Maze task, a procedure designed to explore the role of hippocampus in the formation of spatial memory.

We observed a strong deficit in spatial learning and memory in untreated PKU mice that was completely reversed in HD-Ad treated mice, both at 2 and at 6 months of treatment.

It is known that glutamatergic synaptic is altered in PKU. Acute application of L-Phe at concentrations observed in the PKU brain depressed the glutamatergic synaptic transmission but did not affect GABA receptor activity in cultured neurons (21).

The same authors assessed also the effect of high L- Phe levels *in vivo*, in the forebrain tissue from heterozygous and homozygous PKU mice (22). Consistent with the depressant effects of L-Phe, expression of NMDA receptor NR2A and (RS)–amino-3-hydroxy-5-methyl-4-isoxazolepropionic acid (AMPA) receptor Glu1 and Glu2/3 subunits was significantly increased in PKU mice, whereas expression of NR2B subunit was decreased.

In particular, it is thought that the increase in NR2A/NR2B ratio may contribute to the precocious ageing of PKU brain.

Starting from this, we assessed the expression levels of these receptor subunits in untreated, gene therapy treated and control mice. We confirmed the imbalance in the expression of NMDA and AMPA receptor subunits but obtained significant differences ($p<0.05$) only for NR2B and Glu3. Viral treated mice showed a

normalization of the altered expression of these subunits, supporting a role of Phe in the upregulation/downregulation of NMDA and AMPA receptor subunits.

The activation of NMDA receptors is also known to be involved in long-lasting modifications in synaptic efficiency, namely long-term potentiation (LTP) and long-term depression (LTD), that are classically regarded as the substrate for learning and memory (93). Consistent with the involvement of iGluRs in the cognitive impairment of PKU, we studied NMDA-dependent LTP in the mouse model of PKU. Our results show a severe deficit in LTP in hippocampal slices from homozygous PKU mice that parallels our behavioural studies. Intriguingly, this impairment is restored upon viral treatment, supporting the beneficial effect of gene therapy.

CHAPTER 4- DISCUSSION

During the last year of my PhD, I was involved in another project regarding PKU, that's the characterization of new mutant forms of the PAH enzyme that were identified in PKU patients.

This project is still in progress and our objectives are not only the correlation of the altered chemical physical properties of these mutants to the loss of PAH function but also the identification of new potential therapeutic agents that, stabilizing these mutant forms, may be useful to treat PKU patients.

A general problem faced with in the characterization of mutant forms of hPAH leading to PKU and hyperphenylalaninaemias, has so far been the expression of the full-length mutant enzymes in sufficient quantities.

To date, we have set up the system to produce high amounts of pure proteins for biophysical characterizations.

We have conduced some studies regarding their detailed structural and functional properties that have revealed differences among wild type PAH and its mutants.

BIBLIOGRAPHY

BIBLIOGRAPHY

1. Scriver CR, Kaufman S (2001) Hyperphenylalaninemia: phenylalanine hydroxylase deficiency, in: C.R. Scriver A.L. Beaudet, W.S. Sly, D. Valle, B. Vogelstein (Eds.), The Metabolic and Molecular Bases of Inherited Disease, McGraw_Hill, New York, pp. 1667–1724.

2. Williams RA, Mamotte CDS, Burnett JR (2008) Phenylketonuria: An Inborn Error of Phenylalanine Metabolism. Clin Biochem Rev 29, 31-41.

3. Menkes JH (1967) The pathogenesis of mental retardation in phenylketonuria and other inborn errors of amino acid metabolism. Pediatrics 39:297–308

4. Giannattasio S, Dianzani I, Lattanzi P, Spada M, Romano V, Calı` F, Andria G, Ponzone A, Marra E & Piazza A (2001) Genetic heterogeneity in five Italian regions: analysis of PAH mutations and minihaplotypes. Hum Hered 52, 154–159.

5. Guldberg P, Rey F, Zschocke J, Romano V, Franc¸ois B, Michiels L, Ullrich K, Hoffmann GF, Burgard P, Schmid H et al. (1998) A European multicenter study of phenylalanine hydroxylase deficiency: classification of 105 mutations and a general system for genotype-based prediction of metabolic phenotype. Am J Hum Genet 63, 71–79.

6. Song F, Qu YJ, Zhang T, Jin YW, Wang H, Zheng XY (2005) Phenylketonuria mutations in Northern China. Mol Genet Metab 86, S107–S118.

BIBLIOGRAPHY

7. Okano Y, Asada M, Kang Y, Nishi Y, Hase Y, Oura T, Isshiki G (1998) Molecular characterization of phenylketonuria in Japanese patients. Hum Genet 103, 613–618.

8. Mallolas J, Vilaseca MA, Campistol J, Lambruschini N, Cambra FJ, Estivill X, Mila` M (1999) Mutational spectrum of phenylalanine hydroxylase deficiency in the population resident in Catalonia: genotype–phenotype correlation. Hum Genet 105, 68–73.

9. Zschocke J (2003) Phenylketonuria mutations in Europe. Hum Mutat 21, 345–356.

10. Daniele A, Cardillo G, Pennino C, Carbone MT, Scognamiglio D, Esposito L, Correra A, Castaldo G, Zagari A, Salvatore F (2008) Five human phenylalanine hydroxylase proteins identified in mild hyperphenylalaninemia patients are disease-causing variants. Biochim Biophys Acta 1782, 378–384.

11. Daniele A, Scala I, Cardillo G, Pennino C, Ungaro C, Sibilio M, Parenti G, Esposito L, Zagari A, Andria G, Salvatore F (2009) Functional and structural characterization of novel mutations and genotype–phenotype correlation in 51 phenylalanine hydroxylase deficient families from Southern Italy. FEBS Journal 276 2048–2059.

12. Daniele A, Cardillo G, Pennino C, Carbone MT, Scognamiglio D, Correra A, Pignero A, Castaldo G, Salvatore F (2007) Molecular epidemiology of phenylalanine hydroxylase deficiency in Southern Italy: a 96% detection rate with ten novel mutations. Ann Hum Genet 71, 185–193.

BIBLIOGRAPHY

13. Pey AL, Stricher F, Serrano L, Martinez A (2007) Predicted effects of missense mutations on native-state stability account for phenotypic outcomein phenylketonuria, a paradigm of misfolding diseases. Am. J. Hum. Genet. 81, 1006–1024.

14. Burton BK, Grange DK, Milanowski A, Vockley G, Feillet F, Crombez EA, Abadie V, Harding CO, Cederbaum S, Dobbelaere D et al (2007) The response of patients with phenylketonuria and elevated serum phenylalanine to treatment with oral sapropterin dihydrochloride (6R-tetrahydrobiopterin): a phase II, multicentre, open-label, screening study. Inherit Metab Dis 30, 700–707.

15. Pe´rez-Duen˜ as B, Vilaseca MA, Mas A, Lambruschini N, Artuch R, Go´ mez L, Pineda J, Gutie´rrez A, Mila M, Campistol J (2004) Tetrahydrobiopterin responsiveness in patients with phenylketonuria. Clin Biochem 37, 1083–1090.

16. Blau N, Thony B, Cotton RGH, Hyland K (2001) Disorders of tetrahydrobiopterin and related biogenic amines, in: C.R. Scriver, A.L. Beaudet, W.S. Sly, D. Valle, B. Vogelstein (Eds.), The Metabolic and Molecular Bases of Inherited Disease, McGraw-Hill, New York, pp. 1725–1776.

17. Guthrie R (1996) The introduction of newborn screening for phenylketonuria. A personal history. Eur. J. Pediatr. 155 (Suppl. 1) S4–5.

BIBLIOGRAPHY

18. Park JW, Park ES, Choi EN, Park HY, Jung SC (2009) Altered brain gene expression profiles associated with the pathogenesis of phenylketonuria in a mouse model.Clin Chim Acta. 401(1-2):90-9.

19. Ormazábal A, Artuch R, Vilaseca MA, García-Cazorla A, Campistol J (2004) Pathogenetic mechanisms in phenylketonuria: disorders affecting the metabolism of neurotransmitters and the antioxidant system. Rev Neurol. 39(10):956-61.

20. Shefer S, Tint GS, Jean-Guillaume D, Daikhin E, Kendler A, Nguyen LB, Yudkoff M, Dyer CA (2000) Is there a relationship between 3-hydroxy-3-methylglutaryl coenzyme a reductase activity and forebrain pathology in the PKU mouse? J Neurosci Res 61(5):549-63.

21. Martynyuk AE, Glushakov AV, Sumners C, Laipis PJ, Dennis DM, Seubert CN (2005) Impaired glutamatergic synaptic transmission in the PKU brain. Mol Genet Metab. 86 Suppl 1:S34-42.

22. Glushakov AV, Glushakova O, Varshney M, Bajpai LK, Sumners C, Laipis PJ, Embury JE, Baker SP, Otero DH, Dennis DM, Seubert CN, Martynyuk AE. (2005) Long-term changes in glutamatergic synaptic transmission in phenylketonuria. Brain ;128(Pt 2):300-7.

23. Akeson AL, Berry HK, Brunner RL, Vorhees CV (1979) Brain pyruvate kinase activity in PKU model systems. J Neurochem. Jan;32(1):233-5

BIBLIOGRAPHY

24. Qin M, Smith CB (2007) Regionally selective decreases in cerebral glucose metabolism in a mouse model of phenylketonuria.J Inherit Metab Dis.;30(3):318-25.

25. Hasselbalch S, Knudsen GM, Toft PB, Høgh P, Tedeschi E, Holm S, Videbaek C, Henriksen O, Lou HC, Paulson OB (1996) Cerebral glucose metabolism is decreased in white matter changes in patients with phenylketonuria. Pediatr Res. 40(1):21-4.

26. Wasserstein MP, Snyderman SE, Sansaricq C, Buchsbaum MS (2006) Cerebral glucose metabolism in adults with early treated classic phenylketonuria. Mol Genet Metab. 87(3):272-7

2**7.** Schindeler S, Ghosh-Jerath S, Thompson S, Rocca A, Joy P, Kemp A, Rae C, Green K, Wilcken B, Christodoulou J (2007) The effects of large neutral amino acid supplements in PKU: an MRS and neuropsychological study.Mol Genet Metab. 91(1):48-54

28. Matalon R, Michals-Matalon K, Bhatia G, Burlina AB, Burlina AP, Braga C, Fiori L, Giovannini M, Grechanina E, Novikov P, Grady J, Tyring SK, Guttler F (2007) Double blind placebo control trial of large neutral amino acids in treatment of PKU: effect on blood phenylalanine.J Inherit Metab Dis. 30(2):153-8.

29. Matalon R, Surendran S, Matalon KM, Tyring S, Quast M, Jinga W, Ezell E, Szucs S (2003) Future role of large neutral amino acids in transport of phenylalanine into the brain. Pediatrics. 112(6 Pt 2):1570-4.

BIBLIOGRAPHY

30. Zielke HR, Zielke CL, Baab PJ, Collins RM (2002) Large neutral amino acids auto exchange when infused by microdialysis into the rat brain: implication for maple syrup urine disease and phenylketonuria. J Inherit Metab Dis. 40(4):347-54.

31. Van Spronsen FJ, Smit PG, Koch R. (2001) Phenylketonuria: tyrosine beyond the phenylalanine-restricted diet. J Inherit Metab Dis. 24(1):1-4.

32. Sitta A, Manfredini V, Biasi L, Treméa R, Schwartz IV, Wajner M, Vargas CR (2009) Evidence that DNA damage is associated to phenylalanine blood levels in leukocytes from phenylketonuric patients. Mutat Res. 679(1-2):13-6.

33. Koch R, Hanley W, Levy H, Matalon R, Rouse B, Trefz F, Guttler F, Azen C, Friedman E, Platt L, de la Cruz F (2000) Maternal phenylketonuria: an international study. Mol Genet Metab 71:233–239

34. Dent CE (1957) Relation of biochemical abnormality to development of mental defect in phenylketonuria. Etiologic Factors in Mental Retardation: 23rd Ross Pediatric Research Conference, 1956. Columbus, OH: Ross Laboratories; 32–33

35. Acosta PB, Matalon K, Castiglioni L, et al (2001) Intake of major nutrients by women in the maternal phenylketonuria (MPKU) study and effect on plasma phenylalanine concentrations. Am J Clin Nutr. 73:792–796

36. Unger S, Weigel JF, Stepan H, Baerwald CG (2009) A case of maternal PKU syndrome despite intensive patient counselling. Wien Med Wodenschr 159 (19-20) 507-10

BIBLIOGRAPHY

37. Giovannini M, Verduci ME, Salvatici E, Fiori L, Riva E (2007) Phenylketonuria: dietary and therapeutic challenges. J Inherit Metab Dis 30, 145–152.

38. Lane JD, Schone B, Langenbeck U, Neuho V (1980) Characterization of experimental phenylketonuria. Augmentation of hyperphenylalaninemia with alpha-methylphenylalanine and p-chlorophenylalanine. Biochim. Biophys. Acta 627 144–156.

39. Shedlovsky A, McDonald JD, Symula D, Dove WF (1993) Mouse models of human phenylketonuria. Genetics 134 1205–1210.

40. McDonald JD, Charlton CK (1997) Characterization of mutations at the mouse phenylalanine hydroxylase locus. Genomics 39: 402–405.

41. Cho S, McDonald JD (2001) Effect of maternal blood phenylalanine level on mouse maternal phenylketonuria offspring. Mol. Genet. Metab. 74: 420–425.

42. Pascucci T, Andolina D, Ventura R, Puglisi-Allegra S, Cabib S. (2008) Reduced availability of brain amines during critical phases of postnatal development in a genetic mouse model of cognitive delay. Brain Research 1217:232-8

43. Embury JE, Reep RR, Laipis PJ. (2005) Pathologic and immunohistochemical findings in hypothalamic and mesencephalic regions in the pah (enu2) mouse model for phenylketonuria. Brain Research 58:283-7

44. Embury JE, Charron CE, Martynyuk A, Zori AG, Liu B, Ali SF, Rowland NE, Laipis PJ. (2007) PKU is a reversible neurodegenerative process within the

nigrostriatum that begins as early as 4 weeks of age in Pah (enu2) mice. Brain Research 1127(1):136-50

45. Cabib S, Pascucci T, Ventura R, Romano V, Puglisi_Allegra S (2003) The behavioral profile of severe mental retardation in a genetic mouse model of phenylketonuria. Behav Genet. 33(3): 301-10.

46. Anderson PJ, Wood SJ, Francis DE, Coleman L, Warwick L, Casanelia S, Anderson VA, Boneh A (2004) Neuropsychological functioning in children with early−treated phenylketonuria: impact of white matter abnormalities. Dev Med Child Neurol 46(4):230-8.

47. Smith I, Lobascher ME, Stevenson JE, Wolff OH, Schmidt H, Grubel_Kaiser S, Bickel H (1978) Effect of stopping low phenylalanine diet on intellectual progress of children with phenylketonuria. Br. Med. J. 2: 723-726.

48. Macdonald A, Daly A, Davies P, Asplin D, Hall SK, Rylance G, Chakrapani A (2004) Protein substitutes for PKU: what's new? J Inherit Metab Dis 27(3):363-71. Review.

49. Ikeda K, Schiltz E, Fujii T, Takahashi M, Mitsui K, Kodera Y, Matsushima A, Inada Y, Schulz GE, Nishimura H (2005) Phenylalanine ammonia−lyase modified with polyethylene glycol: potential therapeutic agent for phenylketonuria. Amino Acids 29(3):283-7. Epub 2005 Jun 28.

50. Matalon R, Michals-Matalon K, Bhatia G, Grechanina E, Novikov P, McDonald JD, Grady J, Tyring SK, Guttler F (2006) Large neutral amino

acids in the treatment of phenylketonuria (PKU). J Inherit Metab Dis 29(6):732−8.

51. Fang B, Eisensmith RC, Li XH, Finegold MJ, Shedlovsky A, Dove W, Woo SL (1994) Gene therapy for phenylketonuria: phenotypic correction in a genetically deficient mouse model by adenovirus-mediated hepatic gene transfer. Gene Ther 1:247-254

52. Nagasaki Y, Matsubara Y, Takano H, Fujii K, Senoo M, Akanuma J, Takahashi K, Kure S, Hara M, Kanegae Y, Saito I, Narisawa K (1999) Reversal of hypopigmentation in phenylketonuria mice by adenovirus-mediated gene transfer. Pediatr Res. 45(4 Pt 1): 465-3.

53. Peng H, Armentano D, MacKenzie-Graham L, Shen RF, Darlington G, Ledley FD, Woo SL (1988) Retroviral-mediated gene transfer and expression of human phenylalanine hydroxylase in primary mouse hepatocytes, Proc. Natl. Acad. Sci. USA 85:8146–8150.

54. Liu TJ, Kay MA, Darlington GJ, Woo SL (1992) Reconstitution of enzymatic activity in hepatocytes of phenylalanine hydroxylase deficient mice, Somat. Cell. Mol. Genet. 18:89–96.

55. Mochizuki S, Mizukami H, Ogura T, Kure S, Ichinohe A, Kojima K, Matsubara Y, Kobayahi E, Okada T, Hoshika A, Ozawa K, Kume A (2004) Long-term correction of hyperphenylalaninemia by AAV-mediated gene transfer leads to behavioral recovery in phenylketonuria mice. Gene Ther. 11(13):1081-6

BIBLIOGRAPHY

56. Ding Z, Georgiev P, Thöny B (2006) Administration-route and gender-independent long-term therapeutic correction of phenylketonuria (PKU) in a mouse model by recombinant adeno-associated virus 8 pseudotyped vector-mediated gene transfer.Gene Ther. 13(7):587-93.

57. Brunetti-Pierri N, Clarke C, Mane V, Palmer DJ, Lanpher B, Sun Q, O'Brein W, LeeB (2008) Phenotypic correction of ornithine transcarbamylase deficiency using low dose helper-dependent adenoviral vectors J Gene Med. 10(8):890-6.

58. Jacobs F, Wisse E, De Geest B (2010) The role of liver sinusoidal cells in hepatocyte-directed gene transfer. Am J Pathol. 176(1):14-21.

59. Pastore L, Belalcazar LM, Oka K, Cela R, Lee B et al (2004) Helper-dependent adenoviral vector-mediated long-term expression of human apolipoprotein A-I reduces atherosclerosis in apo E-deficient mice. Gene 327(2): 153-160.

60. Ng P, Parks RJ, Graham FL (2002) Preparation of helper-dependent adenoviral vectors. Methods in molecular medicine 69: 371-388.

61. Rowe WP, Huebner RJ, Gilmore LK, Parrott RH, Ward TG (1953) Isolation of a cytopathogenic agent from human adenoids undergoing spontaneous degeneration in tissue culture. Proceedings of the Society for Experimental Biology and Medicine Society for Experimental Biology and Medicine (New York, NY) 84(3): 570-573.

62. Rekosh DM, Russell WC, Bellet AJ, Robinson AJ (1977) Identification of a

protein linked to the ends of adenovirus DNA. Cell 11(2): 283-295.

63. Anderson CW, Young ME, Flint SJ (1989) Characterization of the adenovirus 2 virion protein, mu. Virology 172(2): 506-512.

64. Matthews DA, Russell WC (1994) Adenovirus protein-protein interactions: hexon and protein VI. The Journal of general virology 75 (Pt 12): 3365-3374.

65. Lukashok SA, Horwitz MS (1998) New perspectives in adenoviruses. Current clinical topics in infectious diseases 18: 286-305

66. Bergelson JM, Cunningham JA, Droguett G, Kurt-Jones EA, Krithivas A et al. (1997) Isolation of a common receptor for Coxsackie B viruses and adenoviruses 2 and 5. Science (New York, NY 275(5304): 1320-1323.

67. Balamotis MA, Huang K, Mitani K (2004) Efficient delivery and stable gene expression in a hematopoietic cell line using a chimeric serotype 35 fiber pseudotyped helper-dependent adenoviral vector. Virology 324(1): 229- 237.

68. Cerullo V, Seiler MP, Mane V, Brunetti-Pierri N, Clarke C et al. (2007) Toll-like receptor 9 triggers an innate immune response to helper-dependent adenoviral vectors. Mol Ther 15(2): 378-385.

69. Stewart PL, Fuller SD, Burnett RM (1993) Difference imaging of adenovirus: bridging the resolution gap between X-ray crystallography and electron microscopy. The EMBO journal 12(7): 2589-2599.

70. Wickham TJ, Mathias P, Cheresh DA, Nemerow GR (1993) Integrins alpha v beta 3 and alpha v beta 5 promote adenovirus internalization but not virus attachment. Cell 73(2): 309-319.

BIBLIOGRAPHY

71. Li E, Stupack D, Bokoch GM, Nemerow GR (1998) Adenovirus endocytosis requires actin cytoskeleton reorganization mediated by Rho family GTPases. Journal of virology 72(11): 8806-8812.

72. Bruder JT, Kovesdi I (1997) Adenovirus infection stimulates the Raf/MAPK signaling pathway and induces interleukin-8 expression. Journal of virology 71(1): 398-404.

73. Matthews DA, Russell WC (1994) Adenovirus protein-protein interactions: hexon and protein VI. The Journal of general virology 75 (Pt 12): 3365-3374.

74. Leopold PL, Kreitzer G, Miyazawa N, Rempel S, Pfister KK et al (2000) Dyneinand microtubule-mediated translocation of adenovirus serotype 5 occurs

after endosomal lysis. Human gene therapy 11(1): 151-165.

75. Angeletti PC, Engler JA (1998) Adenovirus preterminal protein binds to the CAD enzyme at active sites of viral DNA replication on the nuclear matrix. Journal of virology 72(4): 2896-2904.

76. Berk AJ (1986) Adenovirus promoters and E1A transactivation. Annual review of genetics 20: 45-79.

77. Harlow E, Whyte P, Franza BR, Jr., Schley C (1986) Association of adenovirus early-region 1A proteins with cellular polypeptides. Molecular and cellular biology 6(5): 1579-1589.

78. Ben-Israel H, Kleinberger T (2002) Adenovirus and cell cycle control. Front Biosci 7: d1369-1395.

BIBLIOGRAPHY

79. Sundararajan R, Cuconati A, Nelson D, White E (2001) Tumor necrosis factoralpha induces Bax-Bak interaction and apoptosis, which is inhibited by adenovirus E1B 19K. The Journal of biological chemistry 276(48): 45120-45127.

80. Bennett EM, Bennink JR, Yewdell JW, Brodsky FM (1999) Cutting edge: adenovirus E19 has two mechanisms for affecting class I MHC expression. J Immunol 162(9): 5049-5052.

81. Querido E, Blanchette P, Yan Q, Kamura T, Morrison M et al. (2001) Degradation of p53 by adenovirus E4orf6 and E1B55K proteins occurs via a novel mechanism involving a Cullin-containing complex. Genes & development 15(23): 3104-3117.

82. Cepko CL, Sharp PA (1983) Analysis of Ad5 hexon and 100K ts mutants using conformation-specific monoclonal antibodies. Virology 129(1): 137-154.

83. Hasson TB, Soloway PD, Ornelles DA, Doerfler W, Shenk T (1989) Adenovirus L1 52- and 55-kilodalton proteins are required for assembly of virions. Journal of virology 63(9): 3612-3621.

84. Zhang W, Imperiale MJ (2003) Requirement of the adenovirus IVa2 protein for virus assembly. Journal of virology 77(6): 3586-3594.

85. Fessler SP, Young CS (1999) The role of the L4 33K gene in adenovirus infection. Virology 263(2): 507-516.

86. Tollefson AE, Scaria A, Hermiston TW, Ryerse JS, Wold LJ et al. (1996) The

adenovirus death protein (E3-11.6K) is required at very late stages of infection for efficient cell lysis and release of adenovirus from infected cells. Journal of virology 70(4): 2296-2306.

87. Graham FL, Smiley J, Russell WC, Nairn R (1977) Characteristics of a human cell line transformed by DNA from human adenovirus type 5. The Journal of general virology 36(1): 59-74.

88. Yang Y, Nunes FA, Berencsi K, Gonczol E, Engelhardt JF et al. (1994) Inactivation of E2a in recombinant adenoviruses improves the prospect for gene therapy in cystic fibrosis. Nature genetics 7(3): 36

89. Ding Z, Harding CO, Rebuffat A, Elzaouk L, Wolff JA, Thöny B (2008) Correction of murine PKU following AAV-mediated intramuscular expression of a complete phenylalanine hydroxylating system. Mol Ther16(4):673-81.

90. Tang H, Lu D, Pan R, Qin X, Xiong H, Dong J (2009) Curcumin improves spatial memory impairment induced by human immunodeficiency virus type 1 glycoprotein 120 V3 loop peptide in rats. Life Sci. 85 (1-2):1-10

91. Kodirov SA, Takizawa S, Joseph J, Kandel ER, Shumyatsky GP, Bolshakov VY (2006) Synaptically released zinc gates long-term potentiation in fear conditioning pathways. Proc Natl Acad Sci USA 103(41):15218-23

92. Martinez A., Knappskog PM., Olafsdottir S, Doskeland AP, Eiken HG, Svebak RM, Bozzini M, Apold J, Flatmark T (1995) Expression of recombinant human phenylalanine hydroxylase as fusion rotein in Escherichia

coli circumvents proteolytic degradation by host cell poteases Biochem. J. 306: 589–597

93. Bliss TV, Collingridge GL (1993). A synaptic model of memory: long-term potentiation in the hippocampus. Nature 361: 31–9.

This work has been selected for the following poster presentation and oral communication:

Cerreto, M., Nistico, R., Ombrone, D., Ruoppolo, M., Usiello, A., Daniele, A., Pastore, L., Salvatore, F., 2008. Correction of reference memory and synaptic plasticity impairments of PKU mice after a single injection of a helper-dependent adenoviral vector expressing PAH. ***Hum. Gene Ther.*** 19(10): 1119.

Cerreto, M., Nistico, R., Ombrone, D., Ruoppolo, M., Usiello, A., Daniele, A., Pastore, L., Salvatore, F., 2009. Complete reversal of metabolic and neurological symptoms in PKU mice after PAH-HD-Ad vector treatment. ***Hum. Gene Ther.*** 20(11): 1391.